

Lag Phase Is a Distinct Growth Phase That Prepares Bacteria for Exponential Growth and Involves Transient Metal Accumulation

Matthew D. Rolfe,^{a,c} Christopher J. Rice,^a Sacha Lucchini,^a Carmen Pin,^a Arthur Thompson,^a Andrew D. S. Cameron,^e Mark Alston,^{a,d} Michael F. Stringer,^b Roy P. Betts,^b József Baranyi,^a Michael W. Peck,^a and Jay C. D. Hinton^{a,e}

Institute of Food Research, Norwich Research Park, Norwich, United Kingdom^a; Campden BRI, Chipping Campden, Gloucestershire, United Kingdom^b; Department of Molecular Biology and Biotechnology, University of Sheffield, Western Bank, Sheffield, United Kingdom^c; The Genome Analysis Centre, Norwich Research Park, Norwich, United Kingdom^d; and Department of Microbiology, Moyne Institute of Preventive Medicine, School of Genetics & Microbiology, Trinity College, Dublin, Ireland^e

Lag phase represents the earliest and most poorly understood stage of the bacterial growth cycle. We developed a reproducible experimental system and conducted functional genomic and physiological analyses of a 2-h lag phase in *Salmonella enterica* serovar Typhimurium. Adaptation began within 4 min of inoculation into fresh LB medium with the transient expression of genes involved in phosphate uptake. The main lag-phase transcriptional program initiated at 20 min with the upregulation of 945 genes encoding processes such as transcription, translation, iron-sulfur protein assembly, nucleotide metabolism, LPS biosynthesis, and aerobic respiration. ChIP-chip revealed that RNA polymerase was not “poised” upstream of the bacterial genes that are rapidly induced at the beginning of lag phase, suggesting a mechanism that involves *de novo* partitioning of RNA polymerase to transcribe 522 bacterial genes within 4 min of leaving stationary phase. We used inductively coupled plasma mass spectrometry (ICP-MS) to discover that iron, calcium, and manganese are accumulated by *S. Typhimurium* during lag phase, while levels of cobalt, nickel, and sodium showed distinct growth-phase-specific patterns. The high concentration of iron during lag phase was associated with transient sensitivity to oxidative stress. The study of lag phase promises to identify the physiological and regulatory processes responsible for adaptation to new environments.

During batch culture, a typical bacterial growth curve shows five distinct phases of growth: lag phase, the delay before the start of exponential growth; exponential phase, where cell division proceeds at a constant rate; stationary phase, when conditions become unfavorable for growth and bacteria stop replicating (8, 70, 78); death phase, when cells lose viability; and, finally, long-term stationary phase, which can extend for years (27).

The phenomenon of bacterial lag phase was first described at the end of the 19th century, when the “latent period” was described in studies on the effects of temperature on *Salmonella enterica* serovar Typhi (75, 86). Later, in 1949, Monod described lag phase as a process of equilibration that was controlled by an unknown regulatory mechanism (74). Surprisingly, despite a further 60 years of research, this statement remains true. Lag phase is the most poorly understood growth phase, primarily because of a lack of data that describe the underlying physiological and molecular processes.

It has been assumed that lag phase allows the adaptation required for bacterial cells to begin to exploit new environmental conditions (70). This process could include the repair of macromolecular damage that accumulated during stationary phase (21) and the synthesis of cellular components necessary for growth. However, these remain hypothetical possibilities, as the available physiological data simply show that lag-phase bacteria are metabolically active (71). Consequently, there are currently no physiological or biochemical criteria to define lag phase.

Exponential and stationary phases have been studied extensively, representing the processes of cell division and the cessation of division, respectively (78). Exponential growth can occur with a doubling time as short as 20 min for *Salmonella enterica* serovar Typhimurium and requires a number of factors to be present in excess in the growth medium, including sources of carbon, nitrogen, phosphate, and certain trace elements, such as iron. The

physiology of exponential bacterial growth and replication involves multiple rounds of DNA synthesis, coupled with transcription and translation, to synthesize necessary macromolecules. These crucial events are controlled by a variety of gene regulatory processes which are now beginning to be understood by network inference approaches (24). The reason that *Salmonella* enters stationary phase during growth in LB broth is unknown, but the cessation of growth in rich medium has been reported to be caused by both acetate accumulation (119) and carbon starvation (102).

The physiology of bacterial lag phase remains a mystery, but microbiologists have devoted a great deal of effort to measure, model, and predict the duration of bacterial lag time. To improve accuracy, a new predictive model was developed by Baranyi and Roberts to account for the physiological state of the bacterial cell (7). This approach was used to quantify the time taken for “work to be done” during lag phase, which appears to be constant between different bacterial species that are grown under identical conditions (25, 37, 65, 73). The experiments described here are a first step to establishing the nature of this “work” in *S. Typhimurium*.

The relatively low concentrations of bacteria in lag-phase cultures made it challenging to apply functional genomic technologies. This technical difficulty has been overcome in the present

Received 7 September 2011 Accepted 21 November 2011

Published ahead of print 2 December 2011

Address correspondence to Jay C. D. Hinton, jay.hinton@tcd.ie.

M. D. Rolfe and C. J. Rice contributed equally to this article.

Supplemental material for this article may be found at <http://jb.asm.org/>.

Copyright © 2012, American Society for Microbiology. All Rights Reserved.

doi:10.1128/JB.06112-11

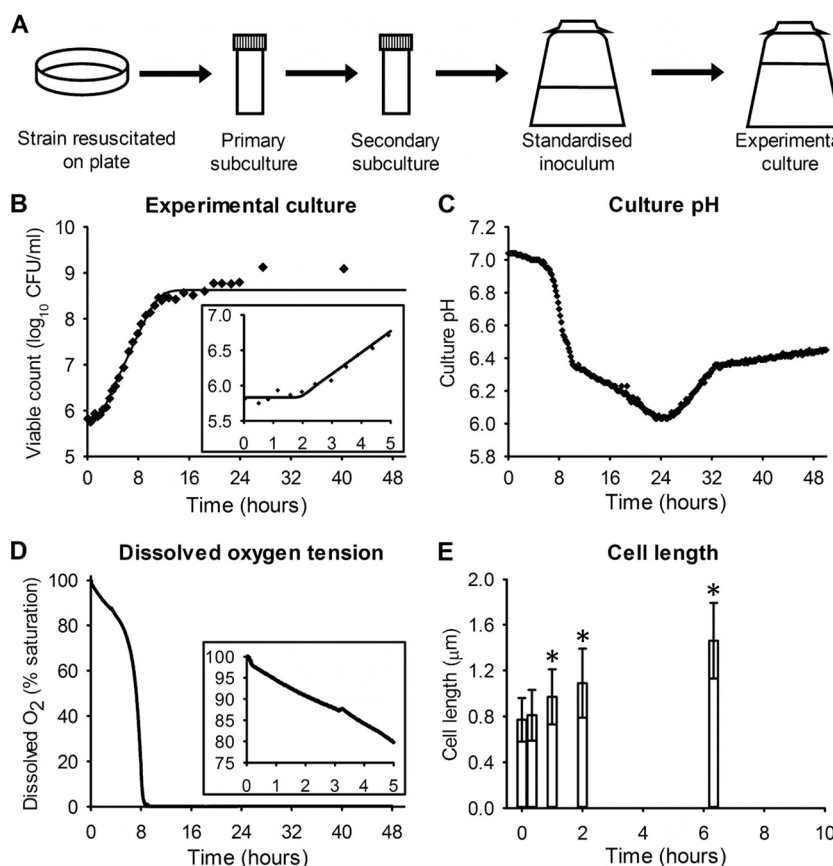


FIG 1 Growth in the experimental system used to characterize the 120-min lag phase of *S. Typhimurium*. (A) Overview of system for obtaining lag-phase cells. See Materials and Methods for details. (B) Growth curve showing lag phase in the experimental culture flask. Lag time was determined to be 2.09 h ($n = 3$). Viable count data for the first 5 h are shown in an inset. (C) Plot of culture pH in the experimental culture. (D) Plot of dissolved oxygen tension in the experimental culture. Oxygen concentrations during the first 5 h are shown in an inset. (E) Cell length in the experimental culture. Statistically significant increases in cell length compared to those in the standardized inoculum (t test; $P < 0.0001$) are shown with an asterisk.

study by the development and use of a simple, robust large-scale system for the functional genomic and biochemical analysis of bacterial lag. Nothing was previously known of the transcriptomic and physiological changes occurring in *Salmonella enterica* serovar Typhimurium cells during lag phase. This paper describes the characterization of the program of transcriptional and physiological events that follow the inoculation of stationary-phase bacteria into fresh medium and represent the earliest stages of bacterial growth.

MATERIALS AND METHODS

Bacterial strains, media, and growth conditions. The parental strain used in this study was *S. Typhimurium* SL1344 (46), and SL1344 *fis::cat* was obtained from C. J. Dorman (57). Strains were grown in LB (pH 7.0) (99) that was filter sterilized (0.22-μm pore size) using Stericup Filter units (Millipore, SCGPU11RE) to minimize potential variations in pH that can be introduced during autoclaving (33). The same batch of powdered medium constituents was used throughout this work to minimize batch-to-batch variation.

Lag phase was studied in 750-ml static cultures grown at 25°C, as shown in Fig. 1A. A standardized inoculum was produced to minimize variation in experimental culture conditions and ensure reproducible population lag times. Strains were streaked from dimethyl sulfoxide (DMSO) stocks at -80°C onto LB agar plates and grown overnight at 37°C. A single colony was taken with an inoculating loop and used to

inoculate a primary subculture of 10 ml LB (pH 7.0) that was grown statically in a 30-ml capped polystyrene universal tube (Fisher Scientific, FB55153) for 48 h at 25°C. An inoculating loop (5 μl) of the stationary-phase primary subculture was used to inoculate a secondary subculture of 10 ml LB (pH 7.0) that was grown statically in a 30-ml capped polystyrene universal tube for 48 h at 25°C.

The standardized inoculum was prepared by adding 200 μl of a 1:100 dilution of the secondary subculture in sterile LB to 500 ml LB (pH 7.0) in a 1-liter Stericup filtration flask. The standardized inoculum in the flask was grown statically at 25°C for exactly 48 h to give a stationary-phase culture (see Fig. S1 in the supplemental material). The experimental flask, consisting of 750 ml LB (pH 7.0) in a 1-liter Stericup filtration flask, was inoculated with 500 μl of this 48-h-old standardized inoculum. Growth was carried out statically at 25°C.

Growth curves and lag-time measurement. Because of inaccurate detection of biomass using optical density measurements and because of variation in bacterial cell size during growth (101), the calculation of lag times using biomass indicators, such as the optical density at 600 nm (OD_{600}), are misleading; viable count measurements are the only accurate way to determine population lag times (104). When measuring growth of the *fis::cat* mutant, parallel wild-type cultures were grown simultaneously to allow direct comparison. Optical density measurements (at OD_{600}) were taken using a SpectraMax Plus spectrophotometer (Molecular Devices).

Growth curve fitting of viable count data was performed using DMFit (www.ifr.ac.uk/safety/DMfit) to measure growth parameters using the

model of Baranyi and Roberts (7). When using DMFit to estimate lag times, the late-stationary-phase time points were excluded from analysis, as they distorted the model fit.

Online measurement of culture pO₂ and pH. Culture pH was monitored using an autoclavable gel-filled electrode (Broadley James), and the dissolved oxygen concentration (pO₂) was monitored using an autoclavable polarographic electrode (Ingold). In both cases, these were connected to an online meter (LH Fermentation, series 2000) that recorded the pH and pO₂ every minute for 48 h.

Inductively coupled plasma mass spectrometry. Published methods (85, 108) were extensively modified to measure levels of cell-associated metals as follows. Bacteria were grown in LB at 25°C in the same static system used elsewhere in this paper (Fig. 1A). For stationary-phase (including the standardized inoculum) and mid-exponential-phase measurements, 15 ml of culture was harvested in 15-ml polypropylene tubes (Greiner Bio One, 188285) prior to centrifugation at 6,300 × g for 10 min at 4°C. These polypropylene tubes cause minimal metal contamination to samples and therefore do not require acid washing (J. Hoogewerff, personal communication). For lag-phase samples, 750 ml of culture was harvested by centrifugation using acid-washed 450-ml centrifuge bottles (Nalgene, 3140-0500) to minimize metal contamination. All further steps were carried out with acid-washed plastic pipette tips. Cell pellets for all time points were washed in 5 ml distilled water (dH₂O) containing 1 mM EDTA (pH 8.0) to bind extracellular metals associated with the cell pellet (3). Cells were washed twice with 5 ml dH₂O and centrifuged (6,300 × g, 10 min, 4°C) between the washes. Pellets were dried in a heat block overnight at 65°C.

Dried cell pellets were digested in 500 µl of 69% Aristar grade nitric acid and 250 µl of 31% Ultrapur hydrogen peroxide (Merck) and left in daylight for 3 days to reduce all organic materials to their constitutive elements. Once digested, each sample was diluted in 6.75 ml of 2% nitric acid containing 1 part per billion (ppb) each of platinum, rhodium, and germanium as internal standards for calibration purposes. Each sample was run in triplicate through an Agilent 7500ce inductively coupled plasma mass spectrometer (ICP-MS). ICP-MS data were statistically filtered using the Grubbs test to remove outlying data (42) ($P < 0.05$). Viable cell count measurements taken at the same time as the ICP-MS samples were used to derive the concentration of metal ions in attomoles per cell.

Microscopy. Cells were taken from the static growth system described above, fixed by the addition of formaldehyde to 4% (vol/vol), and placed on ice for 20 min. The fixed culture was dried onto the surface of a glass microscope slide prior to addition of 10 µl Aqua-Poly/Mount (Polysciences) and a coverslip. Cells were visualized using phase-contrast microscopy on an Olympus BX51 microscope with a UPlanApo Oil Iris ∞/0.17 × 100/1.35 objective (Olympus). Cell sizes were measured from images using AnalySIS Pro v3.2 software.

RNA isolation. For carrying out time course transcriptomic measurements, multiple 750-ml flasks were inoculated at the start of the experiment (time zero). RNA isolation from stationary-phase and exponential-phase cultures was carried out as described previously (56) using protocols available from the Institute of Food Research (IFR) Microarray Facility website (www.ifr.ac.uk/safety/microarrays/). To isolate RNA from lag-phase samples, an entire flask was sacrificed by adding 187.5 ml of ice-cold 5% phenol/95% ethanol (vol/vol) and the flask was placed on ice for 30 min to stabilize the RNA. The 937.5 ml of stabilized culture was centrifuged at 5,500 × g at 4°C for 15 min. Supernatant was poured off, and the pellet was resuspended in the small amount of liquid remaining in the tube. The stabilized cell suspension was then transferred to a 1.5-ml microcentrifuge tube in which a final centrifugation of 6,000 × g for 5 min allowed the removal of the remaining supernatant. RNA was then isolated from these pellets in the same way as they are from exponential- and stationary-phase cultures. This procedure typically yielded between 5 and 10 µg of total RNA from lag-phase cultures harvested at 4 and 20 min after inoculation and up to 50 µg from cultures harvested at later lag-phase

time points. RNA quality was assessed on a 2100 Bioanalyzer (Agilent), and RNA concentration was measured on an ND-1000 spectrophotometer (Nanodrop).

Transcriptomic analysis of RNA samples. Production of labeled cDNA, hybridizations, and analysis of transcriptomic data were carried out with SALSA microarrays as described previously (17). A common-reference experimental design, consisting of Cy5-labeled cDNA and Cy3-labeled genomic DNA (gDNA), was used with each hybridization (106). In total, two biological and two technical replicates were obtained for each of the 11 time points. The median coefficient of variation between biological replicates was 8.9%, while for technical replicates, it was 8.2%.

Transcriptional data were analyzed with GeneSpring 7.3 (Agilent Technologies). Statistical significance was determined with the Benjamini and Hochberg multiple testing correction (false discovery rate of 0.05), and genes that were differentially expressed by more than 2-fold were identified (120). Cluster analysis was carried out within GeneSpring by applying a Pearson correlation. To identify growth-phase-specific marker genes, the transcriptional profiles were split into their respective growth phases: lag phase (4 to 120 min), exponential phase (mid-exponential and late exponential), and stationary phase (inoculum, early stationary phase, and late stationary phase). Growth-phase-specific signature genes were defined as genes that were highly upregulated or downregulated (t test; $P < 0.05$, >2 -fold cutoff) in a single growth phase when all the profiles within that growth phase were compared pairwise to all the profiles in the other two growth phases.

Motif searching. Unbiased motif searching was conducted using Meme version 4.4.0 (4). Gene promoter regions (-300 to +50 bp, relative to the start codon) were searched using the following parameters: motifs could range in size from 10 to 50 bp, each DNA sequence could contain multiple or no motif sites, palindromic and nonpalindromic models were tested, and both the forward and reverse DNA strands were included in searches. Because sigma factors (σ) bind degenerate sites that can be difficult to detect using unbiased motif searching, searches for sigma factor motifs were focused on short promoter regions (-50 to +1 bp, relative to transcription start sites). Sigma factor binding sites are usually composed of two discrete sequence blocks (-10 and -35) with variable spacing between the blocks; thus, preliminary searches for motifs were conducted using BioProspector (67), which is particularly suited to identifying 2-block motifs. BioProspector was used to search for 6- to 12-bp motifs separated by 10 to 25 bp, and this consistently identified a very strong σ^{70} (RpoD) -10 motif. The σ^{70} -35 motif is highly degenerate, necessitating a further refinement of motif searching to test for its presence. To this end, promoter regions were further divided into small segments ranging from -5 to -15 bp (for the -10 motif) and from -25 to -45 bp (for the -35 motif), relative to transcription start sites, and these were searched using Meme with the following parameters: motifs could range in size from 4 to 10 bp, each DNA sequence was expected to contain one sequence matching the motif, and only the forward DNA strand was analyzed. As a positive control, DNA sequences containing the 857 annotated *Escherichia coli* σ^{70} sites were retrieved from RegulonDB 7.0 (31) and searched using these same parameters. Sequence logos were generated using WebLogo (18), and statistically significant differences between logos were calculated and displayed using Two Sample Logo (110).

ChIP-chip. A 1-ml sample of 48-h-old standardized inoculum culture was taken, and chromatin immunoprecipitation with microarray technology (ChIP-chip) was carried out as previously described (68), with the following adjustments. Formaldehyde cross-linking was shortened to 2 min. Bead beating with 100-µm glass beads (Sigma, G4649) was used to lyse the bacterial cells (3 20-s cycles, maximum speed; FastPrep FP120 [Thermo Savant]). During chromatin immunoprecipitation, 20 µl of anti-RNA polymerase β subunit monoclonal antibodies (Neoclone, W0002) was used. Phenylmethylsulfonyl fluoride (PMSF) (Sigma, P7626) was added to each sample after sonication to prevent protein degradation at a final concentration of 1 mM.

Unnormalized ChIP-chip data were analyzed using the ChIPOTle Vi-

sual Basic for applications macro (11). The ChIPOTle macro detected significant RNA polymerase binding peaks by a *t* test ($P < 0.001$) and a 2-fold minimum cutoff threshold. The genomic context of these signal peaks was visualized using the Integrated Genome Browser (IGB) v4.56 (<http://bioviz.org/igb/>).

Assessment of peroxide sensitivity. The sensitivity of *S. Typhimurium* to hydrogen peroxide (H_2O_2) in LB medium was investigated based on a previously published method (6). Briefly, culture was taken at each investigated time point and the initial viable cell count was determined. H_2O_2 was added to the culture at a 6 mM final concentration, and the culture was stored at 4°C for 60 min before the H_2O_2 -treated viable cell count was measured. The fold decrease upon H_2O_2 treatment was calculated by dividing the starting cell count by the H_2O_2 -treated cell count.

Microarray data accession number. The transcriptomic data were deposited in the GEO database (www.ncbi.nlm.nih.gov/geo) under accession number GSE22294.

RESULTS AND DISCUSSION

Characterization of a static system for the reproducible induction of lag phase. Lag time is defined as the initial period in the life of a bacterial population when cells are adjusting to a new environment before starting exponential growth. Many factors influence the duration of lag time, including inoculum size, the physiological history of the cells, and the precise physiochemical environment of both the original and the new growth medium (104). To obtain reproducible lag times, it is important to use a standardized bacterial inoculum and consistent growth conditions. A growth system, based upon culture in LB medium, was developed to generate a robust and reproducible lag phase (Fig. 1A). The standardized inoculum was a 48-h stationary-phase culture of *S. Typhimurium* SL1344 (see Fig. S1 in the supplemental material), and the subsequent 750-ml experimental culture was grown statically at 25°C (Fig. 1B). The combination of 25°C and the lack of agitation was chosen to represent growth of *Salmonella* in food, which can occur at room temperature. This makes our study distinct from the 37°C conditions generally used for infection-related studies with this bacterium (83). The large culture volumes were chosen to provide the quantities of RNA required for transcriptomic analysis of lag phase. This experimental approach is sometimes called “nutrient upshift” or “nutritional upshift” (5, 80); however, this usage is not universal, as these terms can also refer to the transfer of exponential-phase bacteria from minimal to rich media (66).

This static system generated an average lag time of 2.09 h ($n = 3$, standard deviation = 0.32 h), during which cell density remained constant (Fig. 1B), and the cells subsequently entered exponential growth with a doubling time of 0.86 h. During lag phase, there was no significant change in culture pH (Fig. 1C), and this was followed by a substantial decrease in pH during exponential phase. We used a nuclear magnetic resonance (NMR)-based method to measure the concentration of acetate in stationary-phase cultures at 3 mM (data not shown), suggesting that the drop in pH reflected the production of metabolic by-products. The small (10%) reduction in dissolved oxygen tension during lag phase (Fig. 1D) showed that cells were exposed to aerobic conditions throughout lag phase. The subsequent decrease in dissolved oxygen reflected higher oxygen consumption during exponential phase. Cell size measurements identified a statistically significant (*t* test; $P < 0.0001$) 41% increase in the average size of individual cells during lag phase from 0.77 μm to 1.09 μm after 2 h and a further statistically significant (*t* test; $P < 0.0001$) increase to 1.46

μm by mid-exponential phase (Fig. 1E). Thus, although the cells are not dividing during lag phase, they are increasing in size.

Gene expression during lag phase. To measure gene expression, transcriptomic analyses were carried out at six time points during the 2.09-h lag phase of *S. Typhimurium* (4, 20, 40, 60, 90, and 120 min). Additional transcriptional profiles of the standardized inoculum (0 min) and from mid-exponential (6.3 h), late-exponential (10.5 h), early-stationary-phase (15 h), and late-stationary-phase (48 h) cultures allowed the gene expression profile to be measured throughout the growth curve (Fig. 2A; see also Fig. S1 in the supplemental material).

Large-scale transcriptional changes were identified during lag phase when expression levels were compared to those of the standardized inoculum. Using a *t* test ($P \leq 0.05$) and a 2-fold cutoff, expression levels of 1,119 genes changed within 4 min and expression levels of 1,741 genes changed within 20 min of inoculation (Fig. 2B). Virtually all of the transcriptional changes associated with lag phase occurred within 40 min, with very few alterations in gene expression between 40 and 120 min. This suggests that the cells sense their new surroundings remarkably quickly and initiate a novel transcriptional program at the beginning of lag phase. Overall, 2,657 genes (more than half of the genome) showed statistically significant changes in expression between the stationary-phase inoculum and at least one lag-phase time point (see Table S1 in the supplemental material). This reveals the size and scale of the lag-phase-associated transcriptional reprogramming.

The relatedness between the gene expression profiles was assessed at different growth phases (see Fig. S2 in the supplemental material). The lag-phase profiles (20 to 120 min) clustered together and shared similarities with the mid-exponential-phase profile. The first lag-phase sample (4 min) was distinct from all other lag-phase, stationary-phase, and exponential-phase time points, suggesting it represents an adaptation period.

Although the standardized inoculum and late-stationary-phase cultures were both 48-h-old cultures, the physiological states of these two cultures were not directly comparable, as they varied in culture volume (inoculum = 500 ml, late stationary phase = 750 ml) and initial cell density (inoculum = $\sim 10^3$ CFU/ml, late stationary phase = $\sim 6 \times 10^5$ CFU/ml). Therefore, the experimental culture reached stationary phase 8 h earlier than the standardized inoculum culture (Fig. 1B; see also Fig. S1 in the supplemental material). This was reflected by significant differences between the inoculum and late-stationary-phase transcriptional profiles (Fig. 2B).

Functional significance of lag-phase gene expression patterns. Lag-phase transcriptomic data were analyzed in relation to functional categories (55). The numbers of genes changing in each functional category at 4 and 20 min were determined (Fig. 3). The proportions of functional categories changing at the 40-, 60-, 90-, and 120-min time points were broadly identical to that of the 20-min sample (data not shown).

Transcriptional changes during lag phase indicated upregulation of nucleotide metabolism, transcription, lipopolysaccharide (LPS) biosynthesis, and fatty acid biosynthesis. Genes encoding aminoacyl-tRNA synthetases and ribosomal proteins were upregulated during lag phase, reaching exponential-phase expression levels within 20 min. These lag-phase-associated patterns are consistent with the preparation of the bacterial machinery that is required for cellular multiplication during exponential phase.

Identification of lag-phase signature genes. Careful analysis

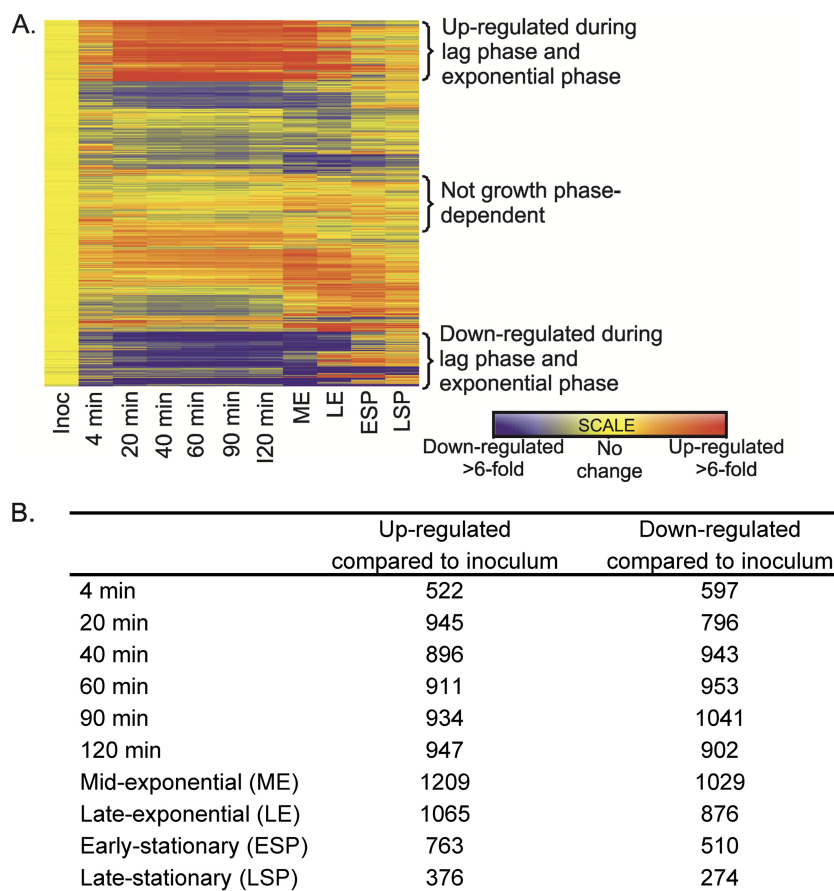


FIG 2 Global picture of gene expression during lag phase of *S. Typhimurium*. (A) Expression of 4,619 SL1344 genes throughout the growth curve of *S. Typhimurium*. Profiles are normalized relative to the standardized inoculum (Inoc). ME, mid-exponential-phase cells; LE, late-exponential-phase cells; ESP, early-stationary-phase cells; LSP, 48-h-old late-stationary-phase cells. Gene expression changes were detected within 4 min. (B) Number of genes that change at each time point. Compared to the standardized inoculum (Inoc) using a *t* test ($P \leq 0.05$, 2-fold cutoff).

revealed a novel set of lag-phase-specific signature genes that showed significant gene expression changes during lag phase when compared to the other growth phases. In total, 20 genes were specifically upregulated during lag phase and 19 genes were downregulated (see Table S2 and Fig. S3 in the supplemental material).

The lag-phase-specific upregulated genes included nine genes implicated in iron uptake or storage, four genes involved in Fe-S cluster synthesis, and two genes involved in manganese uptake (see Table S2 in the supplemental material). The fact that the major classes of genes upregulated during lag phase are involved in metal transport and iron-sulfur cluster formation suggests that accumulation of these metals may be necessary during lag phase to prepare for exponential growth.

The genes that were downregulated during lag phase compared to their expression in the stationary phase and the exponential phase were primarily of unknown function but also included some carbohydrate metabolism genes subject to catabolite control, such as *malT* (15) and *mtlD* (94).

Salmonella essential genes are upregulated during lag phase. To assess the pattern of expression of key physiological processes during lag phase, a published list of essential *Salmonella* Typhi genes previously identified by the TraDIS global mutagenesis technique was used (64). These 356 essential genes are required for growth in LB medium and mediate fundamental biological pro-

cesses, including cell division, DNA replication, transcription, and translation. Three hundred forty-six *S. Typhimurium* genes that were homologous to the essential *S. Typhi* genes were identified (see Table S3 in the supplemental material). The expression patterns of these genes during growth of *S. Typhimurium* SL1344 were compared with those of the stationary-phase inoculum (see Fig. S4 in the supplemental material). Figure 3 shows that the majority of essential *Salmonella* genes were induced during lag phase, with 55% (189 genes) being upregulated at 20 min postinoculation compared to their levels in the stationary-phase inoculum (*t* test; $P < 0.05$ and >2 -fold). A further 5% of essential *Salmonella* genes were upregulated at 60 min postinoculation relative to their levels in the stationary-phase inoculum, making a total of 209 genes (data not shown). The majority of essential genes continued to be highly expressed beyond lag phase, with 68% (234) being upregulated in the mid-exponential-phase transcriptional profile.

Nutrient uptake and metabolic changes during lag phase. LB medium was used for the lag-phase experiments described here. LB contains a low concentration of sugars (<0.1 mM), meaning that several amino acids, including serine, proline, leucine, alanine, arginine, and lysine, are the principal carbon sources (102). Although the activity of core metabolic enzymes in bacteria is not directly related to the levels of individual mRNA transcripts, the

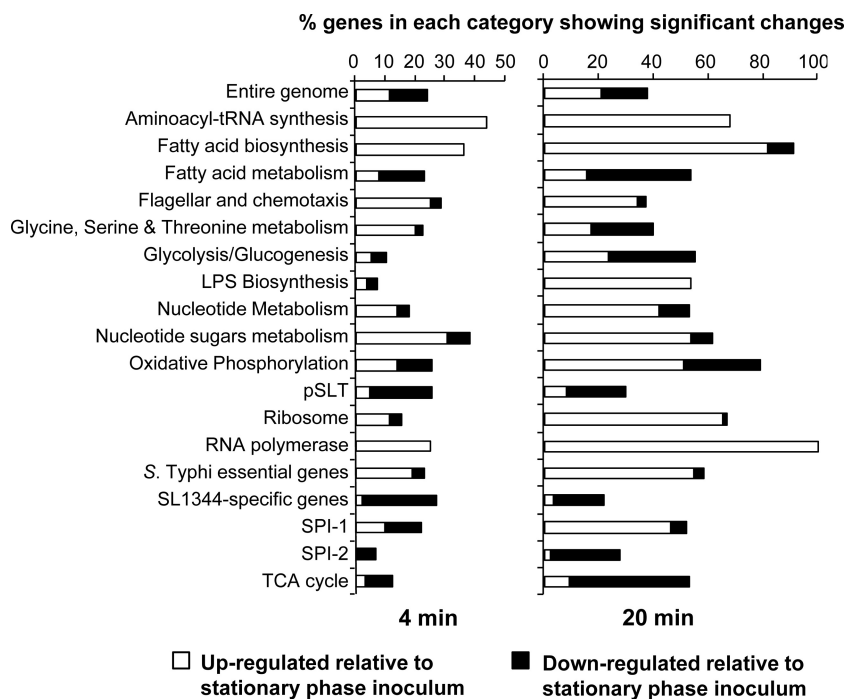


FIG 3 Functional category analysis of lag-phase gene expression (relative to that of the stationary-phase inoculum). Genes that showed statistically significant changes in expression (t test; $P < 0.05$ with a Benjamini and Hochberg multiple testing correction and a 2-fold cutoff) between the stationary-phase inoculum and the 4-min sample and between the stationary-phase inoculum and the 20-min sample were classified into functional categories based on information from the KEGG database (55). Additional categories were SL1344-specific genes (229 genes that are present in *S. Typhimurium* SL1344 but not *S. Typhimurium* LT2) and genes that are essential for growth of *S. Typhi* (346 *S. Typhimurium* homologues of genes identified as essential in *S. Typhi* [64]).

gene expression data can still provide key metabolic insights (23). To gain an overview of the metabolic processes associated with lag phase, the expression of key genes was considered by analyzing raw gene expression profiles (without the use of a stationary-phase sample as a reference sample). In this way, the expression levels of key genes were compared in an unbiased manner.

Most genes encoding glycolytic enzymes showed increased expression during lag phase and exponential phase compared to their levels in the stationary-phase inoculum (see Fig. S5 in the supplemental material). In particular, genes encoding phosphoglucone isomerase (*pgi*), triose phosphate isomerase (*tpiA*), and enolase (*eno*) were upregulated during lag phase. When different enzyme isoforms exist for a glycolytic reaction, upregulation of at least one of the genes encoding an isoform was usually seen. For fructose-bisphosphate aldolase, *fba* was upregulated but *fbaB* appeared repressed. *Fba* is thought to be the main glycolytic enzyme, whereas *FbaB* has been implicated in gluconeogenesis and growth on C3 compounds (100), suggesting that glycolysis is operating in a catabolic direction. For pyruvate kinase, *pykF* showed upregulation while *pykA* was downregulated. *PykF* and *PykA* are both thought to be functional upon growth on glucose; however, *PykF*-specific activity is 15-fold greater than *PykA*-specific activity (88), suggesting that the most highly active form of the enzyme is induced during lag phase. Three phosphoglyceromutase isoforms exist (*GpmA*, *GpmB*, and *GpmM*), and the exact physiological roles of these different isoforms are unclear (28). During lag phase, *gpmA* and *gpmB* were induced while *gpmM* showed no significant changes in expression. The only reaction in glycolysis that did not appear upregulated at the transcriptional level during lag phase was that catalyzed by phosphofructokinase: *pfkA* showed

no change in expression, while *pfkB* was repressed. Over 90% of cellular phosphofructokinase activity is from *PfkA* (63), showing that the most highly active form of enzyme is induced during lag phase.

Transcription of genes encoding the enzymes that mediate gluconeogenesis (*fbp* and *pps*) was downregulated during lag phase. Similarly, the tricarboxylic acid (TCA) cycle and glyoxylate shunt were downregulated during lag-phase and exponential-phase growth, with only the expression of the isocitrate dehydrogenase (*icd*) gene unchanged. It has previously been established that the TCA cycle functions at reduced capacity during rapid growth and that the TCA cycle and glyoxylate shunt were upregulated upon entry to stationary phase in *E. coli* (14). Our gene expression data suggest that glycolysis is the primary metabolic pathway active during lag phase and at all other stages of static growth in LB at 25°C. A preeminent role for glycolysis is counterintuitive because the principal carbon sources in LB are not sugars but amino acids (102).

Overflow metabolism involves the generation of acetate when carbon flux from acetyl coenzyme A (acetyl-CoA) is redirected from the TCA cycle (113) because of reduced expression of TCA enzyme genes in *E. coli* (111). Consequently, we examined the transcriptomic data in relation to acetate production. The enzymes phosphotransacetylase and acetate kinase are responsible for the synthesis of acetate (encoded by the *pta* and *ackA* genes). We observed upregulation of *pta* and *ackA* during lag phase, with a maximal 5-fold induction at 90 min. Taken together, the concomitant downregulation of the TCA cycle and upregulation of acetate synthesis suggest that overflow metabolism is induced during lag phase.

The electron transport chain in *Salmonella* is modular and involves alternative dehydrogenases and terminal oxidoreductases, depending upon the availability of electron donors and electron acceptors (32). In the system studied here, an anaerobic stationary-phase standardized inoculum was transferred into fresh LB medium that had been equilibrated with atmospheric oxygen and, hence, was aerated (Fig. 1D). It was anticipated that aerobic respiration machinery would be synthesized during lag phase. During lag phase, genes encoding the terminal cytochrome oxidase *bo* (*cyoABCD*) were upregulated between 4- and 10-fold and oxygen was consumed (Fig. 1D), indicating that aerobic respiration was taking place. The upregulation of genes encoding NADH dehydrogenases suggest that NADH is the electron donor (*nuoCEFGHIJKN* was upregulated between 2- and 6-fold, and *ndh* was upregulated 5-fold). Anaerobic respiration pathways (for utilizing trimethylamine oxide [TMAO], nitrate, nitrite, DMSO, and fumarate as terminal electron acceptors) were also downregulated during lag phase, indicating that the importance of anaerobic respiration to the cells had now diminished. After the available oxygen was consumed by the bacteria, from late exponential phase onwards, the anaerobic respiration pathways were reestablished.

Phosphate uptake during lag phase. Phosphate is an essential mineral for bacterial growth, required as an integral component of membrane phospholipids, nucleic acids, and nucleotides, and for phosphorylation events within cells. We hypothesized that uptake of phosphate would be important during lag phase to support these processes and examined whether genes involved in phosphate uptake pathways were upregulated during lag phase in *Salmonella*.

Three forms of phosphate can be utilized by *Salmonella*, namely, inorganic phosphate (P_i), organophosphates, and phosphonates. Phosphonates and P_i are taken up directly, while most organophosphates are degraded in the periplasm to yield P_i , which is then transported into the cell (117). The uptake of all phosphate species is controlled by the PhoBR two-component system, which is posttranscriptionally activated under low-phosphate conditions to induce transcription of the phosphate uptake genes (117). The *phoBR* genes showed a transient peak in expression of the PhoBR two-component system at 4 and 20 min into lag phase (Fig. 4A). The major ABC transporter for P_i uptake is encoded by *pstSCAB*, is PhoBR-regulated, and was massively upregulated during lag phase (Fig. 4A); indeed, *pstS* was the most highly upregulated gene (70-fold) 4 min into lag phase. No phosphonate transporter or organophosphate catabolism enzymes were upregulated during lag phase.

The rapid induction of *phoBR* and *pstSCAB* is consistent with a requirement for the uptake of inorganic phosphate during lag phase. A study of *Bacillus licheniformis* also identified upregulation of genes involved in phosphate transport during lag phase (48), suggesting that phosphate uptake may be a universal requirement during lag phase.

Impact of oxidative damage during lag phase. The oxidative stress caused by inoculation from a stationary-phase environment into fresh oxygenated medium impacts growth rate and lag times (19). Oxidative free radicals damage bacteria (12), and OxyR-mediated regulation primarily responds to damage from hydrogen peroxide, sensed by the formation of an intramolecular disulfide bond. Virtually every gene in the OxyR regulon was upregulated during lag phase (at 4 and 20 min) (Fig. 4B). The SoxS regulon, which responds to superoxide, was also induced during

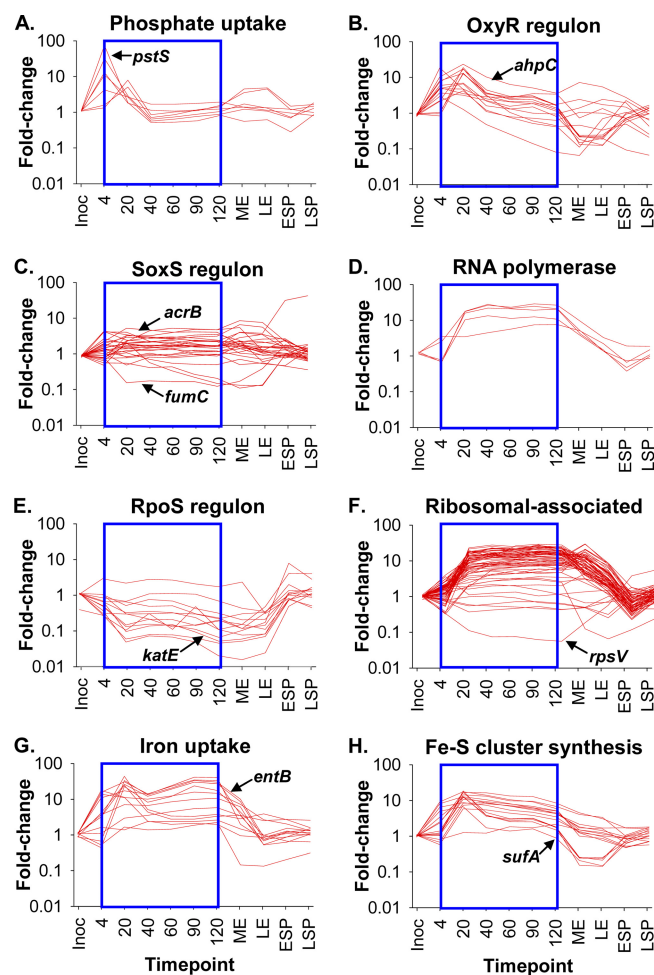


FIG 4 Gene expression profiles of selected gene subsets indicate processes implicated during lag phase. Gene expression is normalized to the standardized inoculum (Inoc), and the lag-phase time points are boxed. Transcriptional profiles are labeled as described in Fig. 2. Various gene subsets are indicated in panels A to H. Phosphate uptake genes are *pstSCAB* and *phoBR*. The OxyR and SoxS regulons of *E. coli* are shown (as defined in EcoCyc [58]). The RNA polymerase category includes *rpoABCZ* and the recycling factor *hepA*. The RpoS regulon was as previously published (49). Ribosomal genes include members of the *rpl*, *rpm*, and *rps* operons. Iron uptake genes are the *ent*, *fep*, and *iro* operons. Fe-S cluster synthesis genes are the *isc* and *suf* operons.

lag phase (Fig. 4C), with most genes in the regulon, including *sodA*, *acnA*, *acrA*, *zwf*, and *nfo*, upregulated at 4 or 20 min and maintained throughout lag phase. Some members of the SoxRS regulon were downregulated during lag phase, notably *fumC* and *fpr*, probably reflecting the upregulation of these genes during stationary phase by σ^{38} . These *Salmonella* data resemble the transcriptome of *E. coli* during the transfer from liquid medium to LB plates at 37°C, which involved the induction of both the SoxRS and OxyR regulons (19).

Repair of damaged cellular components during lag phase. During stationary phase, oxidative damage accumulates in bacteria, with impact on both DNA and proteins (81, 98). Cellular mechanisms are available for repairing DNA damage, but these are downregulated in stationary phase, perhaps to avoid depletion of limited energy resources (98). Consequently, DNA repair mechanisms were expected to be induced during lag phase, par-

ticularly in light of the induction of the OxyR regulon (Fig. 4B). The present study identified only two genes involved in DNA repair that showed lag-phase induction, *nth* (endonuclease III) and *xthA* (exonuclease III). Induction of DNA repair mechanisms was reported during an anaerobic-to-aerobic shift of exponentially growing *E. coli* cells in LB at 37°C (36); however, this induction was not seen here when *S. Typhimurium* was inoculated from a statically grown anaerobic culture at 25°C to fresh medium containing high oxygen concentrations (Fig. 1D). This difference could reflect the lack of oxygen transfer experienced by the static stationary-phase inoculum at 25°C which may limit DNA damage and remove the need for DNA repair during lag phase.

Protein damage accumulates during stationary phase, which can result in the direct oxidation of amino acid residues, protein carbonylation, and aberrant cytoplasmic disulfide bond formation in *E. coli* (21). We wondered whether repair or replacement of damaged proteins would take place during lag phase. Protein carbonylation is irreversible, with carbonylated proteins degraded via HslUV and Lon proteases (30). Gene expression levels of *hslUV* and *lon* showed two peaks at 4 min and 120 min after inoculation, consistent with the possible degradation of carbonylated proteins during lag phase. Aberrant disulfide bonds of cytosolic proteins can be repaired by disulfide reductases, such as thioredoxin and glutaredoxin (90). The genes encoding thioredoxin reductase (*trxB*) and glutaredoxin 1 (*grxA*) were most highly upregulated 20 min after inoculation (5.2-fold and 7-fold, respectively) (see Table S1 in the supplemental material), suggesting that reduction of oxidized disulfide bonds may occur during lag phase. The genes encoding proteins involved in the direct repair of oxidized methionine residues, *msrA* and *msrB* (40), were both induced during stationary phase and downregulated during lag phase and exponential growth. In contrast, transcription of *pcm*, which encodes L-isoaspartate protein carboxylmethyltransferase (114) and is responsible for oxidized aspartate residue repair, was upregulated during lag phase but showed its highest expression in mid-exponential phase. We conclude that the repair of oxidative damage to proteins could be an important process during bacterial lag phase but that the role of DNA repair remains equivocal.

Transcription, RNA polymerase, and sigma factor expression during lag phase. RNA synthesis during lag phase is a prerequisite for the production of proteins required to equip the bacteria for exponential growth. It has been reported that concentrations of core RNA polymerase (RNAP) remain constant during exponential and stationary phase, at around 2,000 complexes per chromosome equivalent in *E. coli* (50), with the activity of RNAP being modulated by competition between sigma factors (39). However, concentrations of RNAP have not been measured during lag phase. Genes encoding RNAP core subunits (α , β , β') share a peak of expression during lag phase (Fig. 4D), implying that increased transcription rates occur during lag phase.

RNAP promoter specificity is mainly controlled by the association of sigma factors with core RNAP. Although sigma factor activity is predominantly controlled at the posttranslational level (43), the expression of sigma factor-encoding genes remains an important factor. The general stress response sigma factor σ^{38} is encoded by *rpoS* (44), which showed a transient transcriptional increase during lag phase, reaching a peak at 20 min (see Fig. S6 in the supplemental material) before decreasing in mid-exponential phase. However, it is unlikely that this leads to a significant increase in the activity of σ^{38} because the RpoS regulon is not acti-

vated during lag phase (Fig. 4E). The housekeeping sigma subunit σ^{70} is encoded by *rpoD*, which showed a 2-fold increase in expression throughout lag phase (see Fig. S6 in the supplemental material), beginning at 20 min and continuing into exponential phase. This pattern is consistent with cells preparing for active growth during lag phase. Expression of *fliA* (σ^{28}) and *rpoN* (σ^{54}) did not change significantly during lag phase, while expression of both *rpoH* (σ^{32}) and *rpoE* (σ^{24}) decreased during lag phase. These data suggest that σ^{70} is the major sigma factor during lag phase.

Ribosomes and translation during lag phase. Ribosome synthesis and translation rates are regulated in a complex fashion to ensure that the cellular ribosome number and protein-synthesizing capability are proportional to the growth rate (60, 115). During lag phase, the number of ribosomes per cell and the translation rate must increase from the low stationary-phase concentration at inoculation to higher (exponential-phase) concentrations at the end of lag phase. The translational ability of a bacterium is dependent upon the number of ribosomes, which is in turn controlled by the levels of rRNA and ribosomal protein in the cell. Because ribosomal protein synthesis is limited by the levels of rRNA (115), measuring the gene expression profiles of rRNA genes provides a convenient way to infer translation rates. Genes encoding ribosomal proteins showed upregulation during lag phase (Fig. 4F); by 20 min into lag phase, the genes were fully upregulated to high levels that were maintained through mid-exponential phase. The rapid upregulation of ribosomal protein synthesis is consistent with a report that *E. coli* rRNA synthesis rates increased within 5 min of nutrient upshift in continuous culture (60), with an accompanying increase in translation. Accordingly, we suggest that considerable protein translation is occurring by 20 min into lag phase.

The role of Fis and the stringent response during lag phase. The nucleoid-associated protein Fis has been reported to regulate many processes relevant to lag phase, such as initiation of DNA replication (26) and transcription of rRNA genes (79, 97) in *E. coli*. At 37°C, Fis shows a peak of expression during late lag and early exponential phase in *Salmonella* (84). This expression was seen in lag phase at 25°C, when increased Fis protein levels were detected 60 min after inoculation, and during exponential growth (see Fig. S7 in the supplemental material).

A *fis* mutant in *Salmonella* has been reported to have an extended lag time and lower growth rate (84). This prompted us to investigate whether Fis is a key regulator that controls lag-phase gene expression. At both 25°C and 37°C, no difference in lag times was seen between SL1344 and an isogenic *fis::cat* mutant using viable-count-based growth curves, although the *fis::cat* mutant did have a lower growth rate than the parental strain at both temperatures (see Fig. S7 in the supplemental material). We conclude that the absence of *fis* does not cause extended lag times and that Fis plays a dispensable role during lag phase.

ppGpp is a bacterial alarmone that can modulate the partitioning of RNAP during the stringent response (89) and that controls a global regulatory system that operates under conditions of nutrient or energy starvation or other environmental stress. We investigated the possibility that ppGpp could be involved in the repartitioning of RNAP during the early stages of lag phase. A *relA spoT* mutant (105), which cannot synthesize ppGpp, does not have an extended lag time (data not shown), suggesting that ppGpp is not playing a critical role during lag phase in rich media.

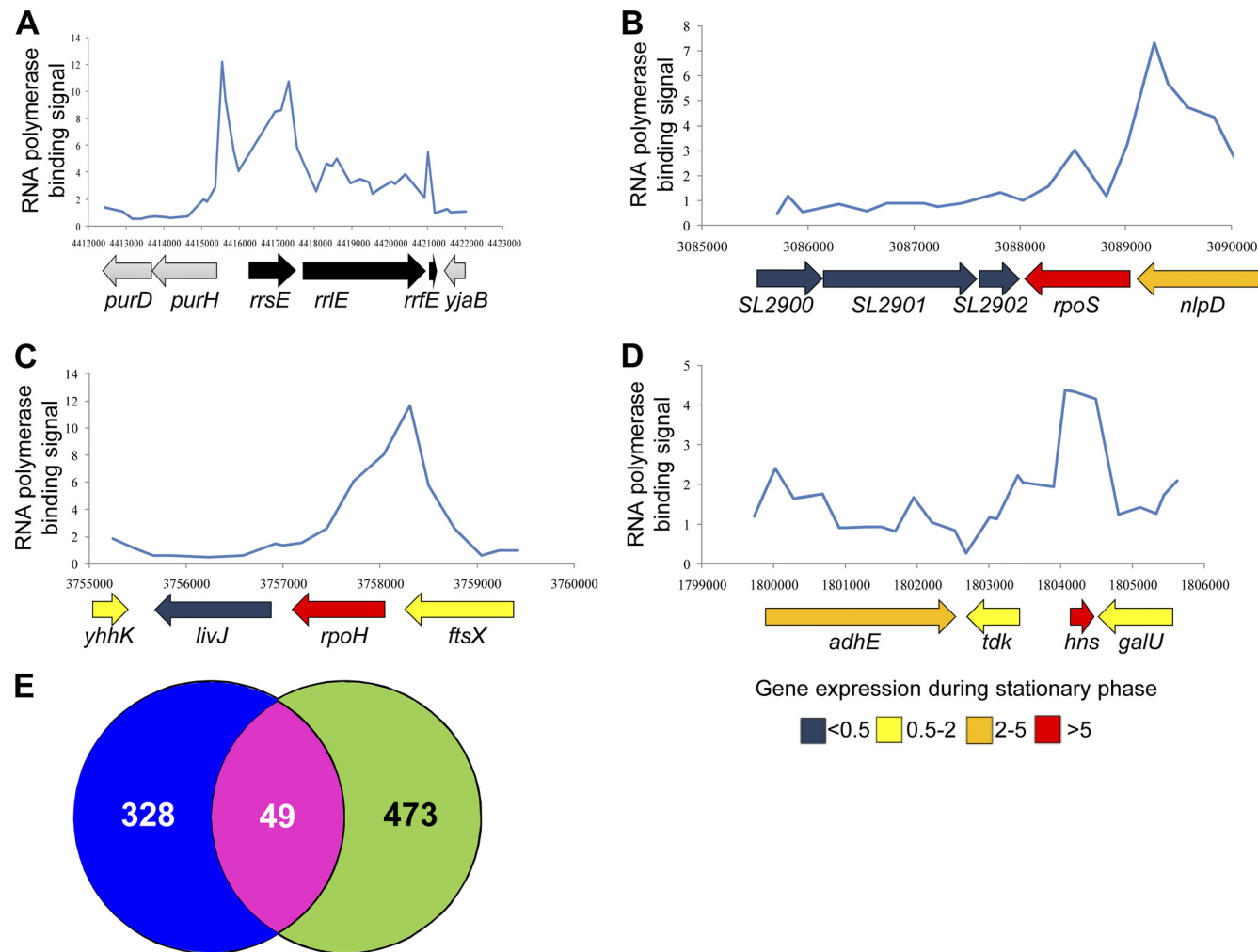


FIG 5 ChIP-chip identification of chromosomal sites associated with RNA polymerase at stationary phase. (A) *rrsE*. (B) *rpoS*. (C) *rpoH*. (D) *hns*. (E) Venn diagram showing the overlap between the 377 gene promoter regions that bind RNA polymerase during stationary phase (left) and the 522 genes highly upregulated during lag phase (4 min postinoculation; right).

RNA polymerase is not poised at lag-inducible promoters.

The rapid transcriptional response of the 522 genes that were upregulated within 4 min of entering lag phase was intriguing. A similar observation was made in the yeast *Saccharomyces cerevisiae*, where 91 genes were upregulated ≥ 4 -fold within the first 3 min of lag phase (93). It was concluded that the rapid transcription during entry into lag phase by yeast reflected prior binding of RNA polymerase II to the relevant promoters during stationary phase without concomitant active transcription. This “poised” state was maintained until transcription was required during lag phase of the yeast. A similar type of binding of RNA polymerase (RNAP) upstream of nontranscribed genes has also been reported in *E. coli* K-12 under conditions of stress (38). Accordingly, we hypothesized that during stationary phase, RNAP could be bound at, or near to, the promoter region of genes that were activated at the beginning of lag phase. We used chromatin immunoprecipitation with microarray technology (ChIP-chip) to test this hypothesis and optimized the lysis procedure for stationary-phase *Salmonella* cells (see Materials and Methods). Using an anti-RNAP antibody that we have validated previously (69), we iden-

tified 377 promoter regions occupied by RNAP during stationary phase (see Table S4 in the supplemental material). These included the major rRNA genes, including *rrsE* and the stationary-phase σ^{38} sigma factor encoded by *rpoS* (Fig. 5A and B). In addition, binding of RNAP was observed in the *rpoH* (σ^{32}) and *hns* genes (Fig. 5C and D). These binding profiles of RNAP are consistent with the high expression of *rpoS*, *rpoH*, and *hns* during stationary phase in *Salmonella* (see Table S1 in the supplemental material).

A comparative analysis of the 377 promoter regions that bound RNAP during stationary phase was undertaken. We determined that less than 13% of the genes that were associated with RNAP at stationary phase were upregulated at 4 min during lag phase (Fig. 5E). These 49 genes include *pnp*, *proV*, and *grxA*. Overall, the ChIP-chip data disprove the hypothesis and show that RNAP is not poised at promoters that are rapidly upregulated during lag phase.

Promoters induced at 4 min have a consensus -35 binding site motif for σ^{70} . In the absence of poised RNAP, we examined other explanations for the upregulation of 522 genes within the first 4 min of lag phase. To investigate whether the relevant pro-

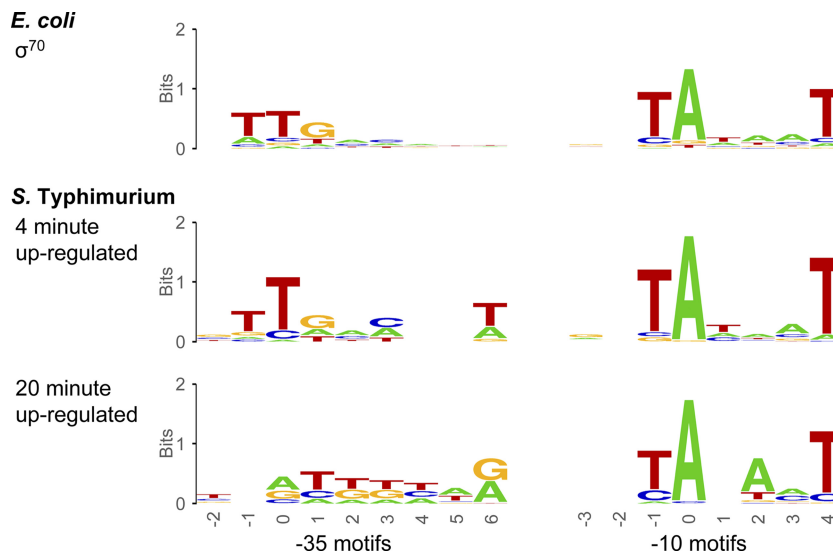


FIG 6 σ^{70} binding site motifs identified in *E. coli* σ^{70} binding regions ($n = 857$) from RegulonDB (31) and in *S. Typhimurium* promoter regions upregulated at 4 min ($n = 43$) and at 20 min ($n = 34$) in lag phase. The numbering of base positions was as previously described (103).

motors share a transcription factor, we searched for the conservation of DNA sequence motifs that could be responsible for transcription factor binding. Transcriptional start sites have been mapped for 43 of the upregulated promoters, and these sites allowed the specific analysis of the 50 bp upstream of the +1 nucleotide. Unbiased motif searching identified two motifs in the promoters upregulated at 4 min, and these motifs closely matched the consensus *E. coli* σ^{70} (*RpoD*) -35 and -10 binding sites (Fig. 6) (103). In addition, the -35 region of the promoters upregulated at 4 min demonstrated a distinctive A+T-rich position 6, which may serve to improve σ^{70} binding specificity or to contribute to DNA deformation by RNA polymerase. Statistical analysis using Two Sample Logo (110) revealed that the 43 promoters that are upregulated at 4 min are significantly enriched for bases matching the -35 binding motif of σ^{70} , whereas the -10 motif is equally strong in all data sets (see Fig. S8 in the supplemental material).

Promoters upregulated at 20 min into lag phase also had strong -10 motifs, but they had no conserved motif at -35 (Fig. 6); weak motifs were identified at the -35 position but were not consistently retrieved when multiple search parameters were tested and so were not considered significant (see Materials and Methods). *S. Typhimurium* promoters that were not induced in lag phase were used as negative controls for motif hunting; these promoters were randomly selected and divided into two sets of 43 promoters to create data sets of similar sizes. Both negative-control sets showed strong matches to the -10 motif of σ^{70} but lacked significant motifs in the -35 region (see Fig. S8 in the supplemental material). These findings lead us to predict that the promoters upregulated at 4 min have significantly better σ^{70} binding sites at the -35 position than the promoters upregulated at 20 min and the negative-control promoters.

Because σ^{70} binding to the -35 region can be functionally replaced by protein-protein contacts between RNA polymerase and transcription factors, many promoters lack σ^{70} binding sites at the -35 region (103). Our discovery of the strong -35 motif in the promoters upregulated at 4 min suggests that the activation of these promoters so early in lag phase reflects the naturally high

affinity that σ^{70} has for these targets and that the promoters that are activated at 4 min are unlikely to require a specific transcription factor to recruit RNAP.

The poor -35 σ^{70} binding motifs associated with genes that were upregulated at 20 min suggest an additional mechanism. 6S is a regulatory RNA that binds to the RNAP σ^{70} holoenzyme (E σ^{70}) to selectively inhibit the transcription of a subset of *E. coli* promoters, which are characterized by a weak -35 σ^{70} binding motif, during stationary phase (13). The inhibition of transcription in stationary phase is relieved upon the introduction of *E. coli* to fresh medium, when the synthesis of 6S-directed product RNA leads to the release of E σ^{70} . A population of free E σ^{70} becomes available within minutes of inoculation of stationary-phase *E. coli* into LB medium (118). The regulatory role of 6S has not been examined in *S. Typhimurium*, but it is likely that if the disassociation of 6S and E σ also occurs within the first few minutes of the start of the *S. Typhimurium* lag phase, free E σ could then become available for transcription. This would explain why the transcription of promoters with weaker -35 σ^{70} binding motifs was not detected until 20 min into lag phase (Fig. 6).

Iron uptake during lag phase. Iron is an essential mineral that is required for bacterial growth, with numerous iron uptake systems available. However, iron acquisition is tightly controlled in bacteria, as excess iron can be toxic (2). High-affinity uptake systems, relying on secretion of siderophores and the reuptake of iron-siderophore complexes into the cell, are required when external iron concentrations are low, while low-affinity iron uptake systems are less well characterized (22). Examination of the transcriptome data showed that expression of the iron uptake machinery was activated during lag phase (Fig. 4G).

Many metabolic and respiratory proteins, such as aconitases (AcnA, AcnB) and succinate dehydrogenase (SdhB), contain Fe-S clusters that are essential for enzyme activity (16, 54, 112). *Salmonella* contains two Fe-S cluster biosynthetic systems, Isc and Suf (92); transcriptional upregulation of genes involved in both systems was seen in early lag phase within 4 to 20 min (Fig. 4H). The expression of genes encoding Isc was maintained through lag

phase, while those encoding Suf decreased, reflecting the different requirements for each system (92).

Iron uptake is controlled by the Fe^{2+} -inducible ferric uptake regulator Fur; the Fur apoprotein binds free intracellular Fe^{2+} to generate the active form of Fur. As the Fe^{2+} -Fur homodimer represses the transcription of Fur-responsive genes (72), decreased levels of Fe^{2+} -Fur are likely to be responsible for the higher expression of iron acquisition systems (109). These data prompted us to measure levels of cell-associated iron during growth as detailed below.

Lag phase is characterized by the specific but transient uptake and loss of metal ions. Metals play a critical role in bacterial life as essential micronutrients fundamental to central metabolic processes and are required for pathogenic virulence (1, 41, 45). Intricate machinery has evolved to finely tune the intracellular concentration of metals to achieve metal homeostasis and prevent metal toxicity (35). Because many metal transporters were specifically induced during lag phase, we investigated whether specific metals were accumulated during lag phase. It is now possible to audit many metals simultaneously using the highly sensitive inductively coupled plasma mass spectrometry (ICP-MS) method, which simultaneously detects 36 metals associated with bacterial cells (85).

Quantitative assessment of the metallome of *S. Typhimurium* showed that maximal cell-associated concentrations of manganese, calcium, and iron occurred during lag phase. The highest concentrations of manganese (Fig. 7A) and calcium (Fig. 7B) were detected at 4 min postinoculation (2.9×10^{-19} moles per cell and 7.16×10^{-16} moles per cell, respectively). The accumulation of manganese correlated with the upregulation of the *sitABCD* transporter genes (Fig. 7C). For iron, the correlation with the expression of the relevant transporter genes is less clear-cut, but it is evident at the 4-min time point. We speculate that changes in cell-associated metal concentrations could regulate the activity of metabolic enzymes. For instance, phosphoglycerate mutase (discussed earlier) contains three isoforms, GpmA, GpmB, and GpmM (29); as GpmM requires a Mn^{2+} cofactor, its activity could be influenced by increased cell-associated Mn^{2+} concentrations. The precise role of ChaA in calcium transport remains controversial (77), but we note that the expression of *chaA* correlates with cell-associated calcium levels. The huge increase in calcium may have a physiological role during lag phase, as it has been suggested that calcium is involved in the motility, chemotaxis, and cytoskeletal organization of *E. coli* (47). Subsequently, calcium and manganese concentrations decreased dramatically during mid-exponential and stationary phases of growth, suggesting that the physiological need for these metals is highest during lag phase and raising the possibility that these metals play an important role in the transition from lag phase into exponential growth.

Iron accumulation showed a transient pattern during lag phase, with the highest cellular concentration (4.1×10^{-18} moles per cell) during the earliest stages of lag. Iron accumulation correlates with expression of the dedicated iron transport machinery, which increases during lag phase (Fig. 7C). We suggest that iron uptake is required during the earliest stages of growth for the assembly of iron cofactors and Fe-S clusters that are associated with essential metabolic machinery (51).

The cell-associated concentrations of several other metals, including molybdenum, cobalt, and nickel, were reduced during lag phase (Fig. 7; see also Fig. S9 in the supplemental material). Mo-

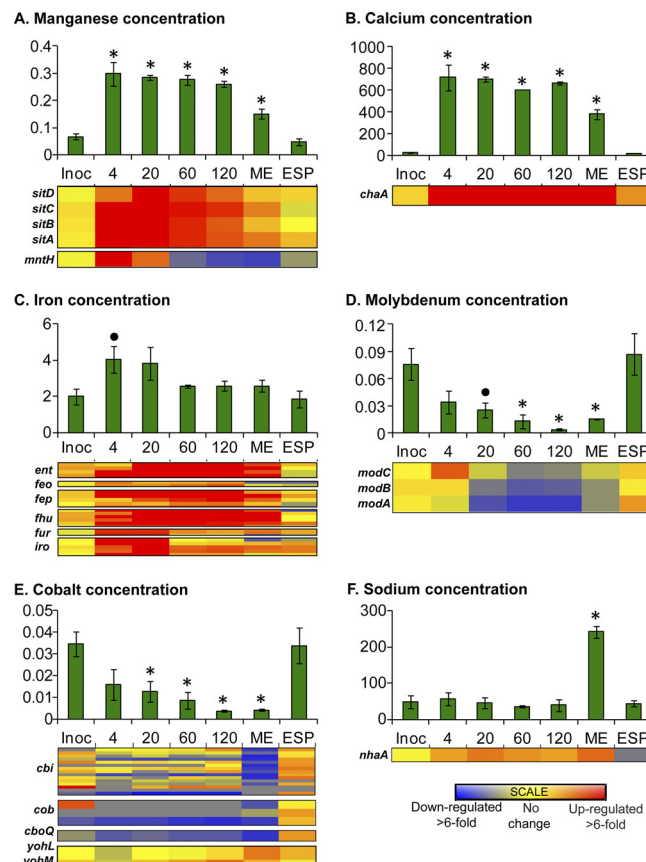


FIG 7 *S. Typhimurium* cell-associated metal ion accumulation (attomoles per cell) was measured with ICP-MS at different growth phases, and the corresponding expression levels of genes encoding metal uptake machinery are shown. Profiles for the uptake of manganese (A), calcium (B), iron (C), molybdenum (D), cobalt (E), and sodium (F) are indicated. Gene expression is normalized to the standardized inoculum (Inoc), and the time points are labeled as in Fig. 2. Statistically significant changes in cell-associated metal concentrations from those for the standardized inoculum are indicated (*t* test; *, $P < 0.05$; ●, $P < 0.1$). References for each transporter system are listed in Table S5 in the supplemental material.

lybdenum is used as a cofactor for a number of enzymes involved in bacterial oxidation/reduction reactions, primarily under anoxic conditions (59). In the present study, maximal accumulation (9×10^{-20} moles per cell) of molybdenum occurred during anaerobic stationary phase, and the concentration of molybdenum was reduced during the oxygen upshift associated with lag phase (Fig. 7D).

A similar pattern was observed for nickel (see Fig. S9 in the supplemental material) and cobalt (Fig. 7E), which were both maximally accumulated at stationary phase, correlating with the highest expression of their respective transporter genes (95). The cell-associated concentrations of cobalt and nickel decreased upon entry into lag phase, coinciding with downregulation of the relevant transport machinery. It was recently reported that elevated nickel levels can disrupt iron homeostasis (116). We note that increased levels of iron are associated with a decreased concentration of nickel during lag phase (Fig. 7C; see also Fig. S9 in the supplemental material), consistent with a homeostatic mechanism that ensures that bacterial cells do not contain high concentrations of both nickel and iron simultaneously. We observed a

marked upregulation of *yohM* (*rcaA*), which encodes the $\text{Ni}^{2+}/\text{Co}^{2+}$ efflux protein, and its regulator, YohL (RcnR), at later stages of lag phase (starting at 60 min postinoculation) (Fig. 7) (52, 53, 96). Nickel has a biological role as a cofactor for anaerobically expressed NiFe hydrogenases (76, 121). Like molybdenum, the gradual removal of cell-associated nickel and cobalt coincided with an oxygen upshift during lag phase. This would be consistent with the cytotoxicity of nickel and cobalt in the presence of intracellular peroxide (34).

We noted that the cell-associated concentrations of sodium (Fig. 7F) and magnesium (see Fig. S9B in the supplemental material) were maximal in mid-exponential phase (2.4×10^{-16} and 8×10^{-17} moles per cell, respectively), suggesting that these metals play a specific role during exponential growth. Examination of the transcription of genes encoding magnesium transporters (*corA*, *mgtA*, and *mgtBC*) revealed that *mgtA* showed a peak of expression during early lag phase when compared with the inoculum (5.4-fold upregulated) and late exponential phase (7.8-fold upregulated) (see Table S1 in the supplemental material), suggesting that MgtA could be responsible for the increase in magnesium concentration seen during exponential phase. The *corA* gene was most highly expressed during stationary phase, while *mgtBC* showed highest expression (5.5- to 7.8-fold) during early lag phase. The gene encoding the sodium/proton transporter *nhaA* was most highly expressed (2.5-fold upregulated) during mid-exponential growth, correlating with the highest concentration of sodium ions. The raised level of cell-associated sodium ions could balance a rise in the external proton concentration caused by an increase in proton motive force during exponential growth. Other metals that have no known physiological role in bacteria accumulated during lag phase. These include strontium, chromium, and aluminum (see Fig. S9 in the supplemental material). This may reflect promiscuity between metal transporters that results in the coaccumulation of several metals.

Lag-phase cells show increased sensitivity to hydrogen peroxide. The observation that the cell-associated levels of both iron and manganese rise at the earliest stage of lag phase is intriguing. Increased intracellular pools of free iron are known to stimulate Fenton chemistry and cause sensitivity to oxidative stress (107), while manganese ions can protect against oxidative stress by substituting for iron in mononuclear enzymes (3). Our data show that the cell-associated ratios of iron to manganese were 35.4 (late stationary phase) and 13.9 (at 4 min postinoculation). In contrast, the ratio of iron to manganese in *E. coli* cells grown in minimal medium is 66.66 (3). We considered the possibility that the relative increase in manganese levels during lag phase could serve to dampen the oxidative damage associated with inoculation into aerated medium. We hypothesized that the presence of increased intracellular iron would induce a short-lived peroxide sensitivity during lag phase and that this could be ameliorated by the presence of manganese. Figure 8 shows that a transient sensitivity to oxidative stress was seen at 4 min and 20 min postinoculation, correlating with the highest concentration of bacterium-associated iron. This sensitivity to hydrogen peroxide coincides with the induction of the OxyR regulon at 4 min and 20 min (Fig. 4B) and suggests that oxidative damage is caused by the combination of increased intracellular iron and the newly available oxygen. The bacterial cells became more resistant to the hydrogen peroxide by 60 min postinoculation, coinciding with a tailing off of the transcription of genes within the OxyR regulon and the continued

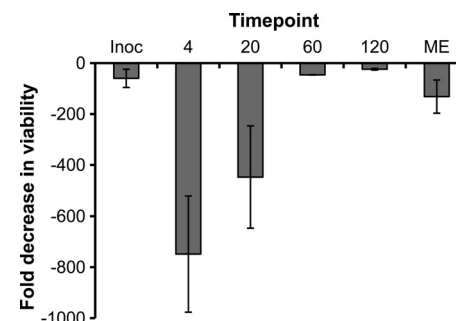


FIG 8 Lag-phase *Salmonella* shows increased sensitivity to hydrogen peroxide. Culture was taken at the indicated time points and exposed to H_2O_2 for 60 min, and the fold decrease in cell viability is shown. The 4-min lag-phase culture showed a statistically significant difference (*t* test; $P < 0.05$) in hydrogen peroxide sensitivity when compared to the sensitivities of the inoculum, 60-min, 120-min, and mid-exponential-phase cultures.

high expression of iron import genes. We propose a model whereby *S. Typhimurium* resists oxidative stress during early lag phase in aerobic environments by binding preexisting pools of intracellular iron before actively accumulating additional iron from the medium after successful adaptation. Further phenotypic data are required to confirm this hypothesis.

Conclusions. This study has characterized the key processes that occur during bacterial lag phase (Fig. 9). The evidence suggests that the cells sense their new surroundings remarkably quickly and initiate transcription during early lag phase to prepare for exponential growth. The detailed transcriptomic analysis of lag phase reported here should support the future identification of the underlying regulatory mechanisms that choreograph the transitions from stationary to lag phase and from lag to exponential phase. These systems are likely to complement the established roles played by transcription factors during stationary phase (e.g., RpoS [61]) and by repressors during exponential growth (e.g., StpA [68]).

Previously, we performed a network-based study of lag phase in *E. coli* K-12 cells grown under similar growth conditions (87). It contained uncorroborated transcriptomic data that identified 186 genes that were differentially expressed during lag phase; the majority of these genes (79%) showed a pattern comparable to that of genes in *S. Typhimurium* (at 60 min postinoculation). This suggests that the physiological processes occurring during lag phase are broadly similar in *E. coli* and *Salmonella*.

Our study reveals that the bacterial transcriptional machinery of a 2-day-old stationary-phase bacterial cell mediates radical changes in gene expression within 4 min of entering a new environment and represents a period of adaptation between the stationary-phase and lag-phase transcriptional programs. RNAP binds nonspecifically to DNA as the growth rate of *E. coli* is reduced (62), suggesting that there is a relatively high concentration of free RNAP present in stationary-phase cultures. Our ChIP-chip data show that RNAP is associated with hundreds of chromosomal regions and confirms reports that active transcription continues during stationary phase (91). It is clear that the promoters of the genes that are upregulated at 4 min into lag phase share an extremely strong σ^{70} binding motif. The fact that RNAP is not bound at these promoters at stationary phase suggests that the enzyme must partition extremely rapidly to initiate high levels of

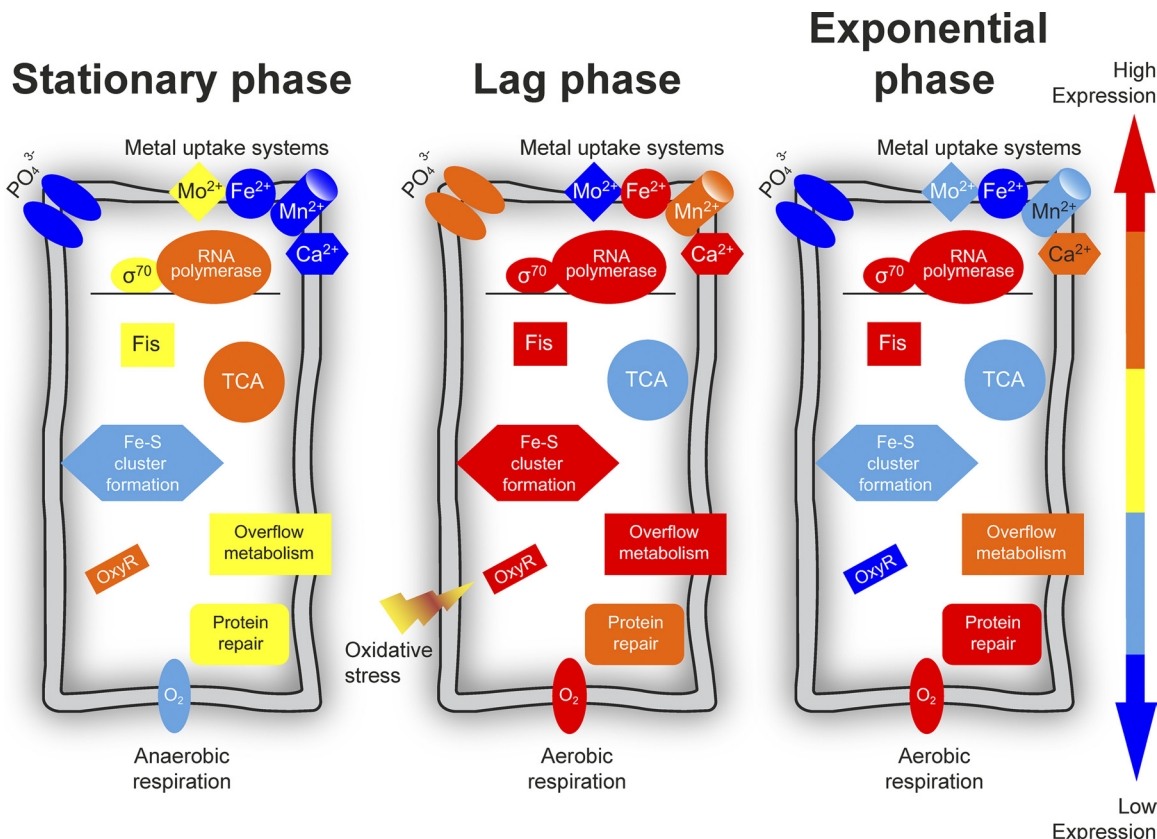


FIG 9 Model showing the major physiological processes occurring during lag phase, exponential phase, and stationary phase of *S. Typhimurium* in the static system in LB at 25°C. Each symbol represents groups of functionally related proteins and is colored according to the level of expression of the appropriate genes under each growth condition. Blue shows that the relevant genes are expressed at low levels, yellow shows genes expressed at medium levels, and red shows genes expressed at high levels in each growth phase.

transcription within 4 min of entering a permissive growth environment.

Systems such as iron and phosphate uptake, Fe-S cluster formation, and oxidative stress deserve intensive investigation to fully determine their roles in lag phase. Our discovery that iron and manganese are accumulated by *S. Typhimurium* during lag phase constitutes strong phenotypic confirmation of the transcriptional patterns of metal transport genes. Taken together, these findings reveal important features of metabolism during the earliest stage of bacterial growth, and they led us to identify a transient sensitivity to oxidative damage during early lag phase.

Until now, the study of lag phase has received more attention in eukaryotes than in prokaryotes. Transcriptional analysis of *Saccharomyces cerevisiae* identified genes that show lag-phase-dependent expression when compared to a stationary-phase inoculum. During early lag phase, genes involved in translation, protein folding, modification, translocation and degradation, ribosome biogenesis, transcription, RNA processing, cell polarity, cell division, and cell cycle control were induced (9, 10). The present study shows that most of these fundamental classes of genes are also upregulated during bacterial lag phase.

Stationary phase precedes the “death phase” and the end of bacterial life. The fact that stationary-phase cultures of *E. coli* contain a mixture of damaged and healthy bacteria (20) suggests that conditional senescence and aging occur in both prokaryotic and

eukaryotic microorganisms (82). However, there is an important and fundamental difference between the mandatory aging of eukaryotic cells and the conditional senescence of bacteria: the latter is a reversible process. When stationary-phase bacterial cells are subcultured into fresh medium, they enter lag phase, halt the degenerative process, and prepare for exponential division. Our data are consistent with lag phase representing the rejuvenation of bacterial life that accompanies the repair of oxidative damage and the development of the intracellular macromolecular stores needed for optimal growth.

It seems fitting that as *Salmonella* was the first bacterium in which lag phase was studied (75), it is now the first Gram-negative bacterium to be understood at the level of global gene expression during lag phase.

ACKNOWLEDGMENTS

M.D.R. (BBS/S/N/2003/10520) and C.J.R. (BBS/S/M/2006/13059) were supported by Biotechnology and Biological Sciences Research Council (BBSRC) Collaborative Awards in Science and Engineering (CASE) studentships that were cofunded by Campden BRI. We are grateful for financial support from the BBSRC Core Strategic Grant.

We thank Tyrrell Conway and Werner Goebel for their metabolic insights, David Richardson and Charles Dorman for their helpful suggestions, Isabelle Hautefort for assistance with light microscopy work, and other members of the Hinton lab for their encouragement. We are grateful to Yvette Wormstone for printing microarrays, to Paul Pople for as-

sistance with graphics, and to Jurian Hoogewerf and John Eagles for excellent ICP-MS analyses.

REFERENCES

- Agranoff D, Krishna S. 2004. Metal ion transport and regulation in *Mycobacterium tuberculosis*. *Front. Biosci.* 9:2996–3006.
- Andrews SC, Robinson AK, Rodriguez-Quinones F. 2003. Bacterial iron homeostasis. *FEMS Microbiol. Rev.* 27:215–237.
- Anjem A, Varghese S, Imlay JA. 2009. Manganese import is a key element of the OxyR response to hydrogen peroxide in *Escherichia coli*. *Mol. Microbiol.* 72:844–858.
- Bailey TL, Williams N, Misleh C, Li WW. 2006. MEME: discovering and analyzing DNA and protein sequence motifs. *Nucleic Acids Res.* 34:W369–W373.
- Ball CA, Osuna R, Ferguson KC, Johnson RC. 1992. Dramatic changes in Fis levels upon nutrient upshift in *Escherichia coli*. *J. Bacteriol.* 174: 8043–8056.
- Bang IS, Frye JG, McClelland M, Velayudhan J, Fang FC. 2005. Alternative sigma factor interactions in *Salmonella*: sigma(E) and sigma(H) promote antioxidant defences by enhancing sigma(S) levels. *Mol. Microbiol.* 56:811–823.
- Baranyi J, Roberts TA. 1994. A dynamic approach to predicting bacterial growth in food. *Int. J. Food Microbiol.* 23:277–294.
- Baranyi J, Roberts TA. 2000. Principles and application of predictive modeling of the effects of preservative factors on microorganisms, p 342–358. In Lund BM, Baird-Parker TC, Gould GW (ed), *The microbiological safety and quality of food*. Aspen, Gaithersburg, MD.
- Brejning J, Arneborg N, Jespersen L. 2005. Identification of genes and proteins induced during the lag and early exponential phase of lager brewing yeasts. *J. Appl. Microbiol.* 98:261–271.
- Brejning J, Jespersen L, Arneborg N. 2003. Genome-wide transcriptional changes during the lag phase of *Saccharomyces cerevisiae*. *Arch. Microbiol.* 179:278–294.
- Buck MJ, Nobel AB, Lieb JD. 2005. ChIPOTle: a user-friendly tool for the analysis of ChIP-chip data. *Genome Biol.* 6:R97.
- Cabiscol E, Tamarit J, Ros J. 2000. Oxidative stress in bacteria and protein damage by reactive oxygen species. *Int. Microbiol.* 3:3–8.
- Cavanagh AT, Klocko AD, Liu X, Wasserman KM. 2008. Promoter specificity for 6S RNA regulation of transcription is determined by core promoter sequences and competition for region 4.2 of sigma70. *Mol. Microbiol.* 67:1242–1256.
- Chang D, Conway T. 2005. Metabolic genomics. *Adv. Microb. Physiol.* 50:1–39.
- Chapon C, Kolb A. 1983. Action of CAP on the *malT* promoter *in vitro*. *J. Bacteriol.* 156:1135–1143.
- Cheng VW, Ma E, Zhao Z, Rothery RA, Weiner JH. 2006. The iron-sulfur clusters in *Escherichia coli* succinate dehydrogenase direct electron flow. *J. Biol. Chem.* 281:27662–27668.
- Clements MO, et al. 2002. Polynucleotide phosphorylase is a global regulator of virulence and persistency in *Salmonella enterica*. *Proc. Natl. Acad. Sci. U. S. A.* 99:8784–8789.
- Crooks GE, Hon G, Chandonia JM, Brenner SE. 2004. WebLogo: a sequence logo generator. *Genome Res.* 14:1188–1190.
- Cuny C, Lesbats M, Dukan S. 2007. Induction of a global stress response during the first step of *Escherichia coli* plate growth. *Appl. Environ. Microbiol.* 73:885–889.
- Desnues B, et al. 2003. Differential oxidative damage and expression of stress defence regulons in culturable and non-culturable *Escherichia coli* cells. *EMBO Rep.* 4:400–404.
- Dukan S, Nystrom T. 1998. Bacterial senescence: stasis results in increased and differential oxidation of cytoplasmic proteins leading to developmental induction of the heat shock regulon. *Genes Dev.* 12: 3431–3441.
- Earhart CF. 1996. Uptake and metabolism of iron and molybdenum, p 1075–1090. In Neidhardt FC, et al (ed), *Escherichia coli and Salmonella: cellular and molecular biology*, 2nd ed, vol 2. ASM Press, Washington, DC.
- Eisenreich W, Dandekar T, Heesemann J, Goebel W. 2010. Carbon metabolism of intracellular bacterial pathogens and possible links to virulence. *Nat. Rev. Microbiol.* 8:401–412.
- Faith J, et al. 2007. Large-scale mapping and validation of *Escherichia coli* transcriptional regulation from a compendium of expression profiles. *PLoS Biol.* 5:54–66.
- Fernández P, George S, Sills C, Peck M. 1997. Predictive model of the effect of CO₂, pH, temperature and NaCl on the growth of *Listeria monocytogenes*. *Int. J. Food Microbiol.* 37:37–45.
- Filutowicz M, Ross W, Wild J, Gourse RL. 1992. Involvement of Fis protein in replication of the *Escherichia coli* chromosome. *J. Bacteriol.* 174:398–407.
- Finkel SE. 2006. Long-term survival during stationary phase: evolution and the GASP phenotype. *Nat. Rev. Microbiol.* 4:113–120.
- Foster JM, et al. 2010. Evolution of bacterial phosphoglycerate mutases: non-homologous isoform enzymes undergoing gene losses, gains and lateral transfers. *PLoS One* 5:e13576.
- Fraser HI, Kvaratskhelia M, White MF. 1999. The two analogous phosphoglycerate mutases of *Escherichia coli*. *FEBS Lett.* 455:344–348.
- Fredriksson A, Ballesteros M, Dukan S, Nystrom T. 2005. Defense against protein carbonylation by DnaK/DnaJ and proteases of the heat shock regulon. *J. Bacteriol.* 187:4207–4213.
- Gama-Castro S, et al. 2011. RegulonDB version 7.0: transcriptional regulation of *Escherichia coli* K-12 integrated within genetic sensory response units (Gensor Units). *Nucleic Acids Res.* 39:D98–D105.
- Gennis RB, Stewart V. 1996. Respiration, p 217–261. In Neidhardt FC et al (ed), *Escherichia coli and Salmonella: cellular and molecular biology*, 2nd ed, vol 1. ASM Press, Washington, DC.
- George SM, Richardson LCC, Peck MW. 1996. Predictive models of the effect of temperature, pH and acetic and lactic acids on the growth of *Listeria monocytogenes*. *Int. J. Food Microbiol.* 32:73–90.
- Geslin C, Llanos J, Prieur D, Jeanthon C. 2001. The manganese and iron superoxide dismutases protect *Escherichia coli* from heavy metal toxicity. *Res. Microbiol.* 152:901–905.
- Giedroc DP, Arunkumar AI. 2007. Metal sensor proteins: nature's metallocregulated allosteric switches. *Dalton Trans.* 7:3107–3120.
- Gifford CM, Blaisdell JO, Wallace SS. 2000. Multiprobe RNase protection assay analysis of mRNA levels for the *Escherichia coli* oxidative DNA glycosylase genes under conditions of oxidative stress. *J. Bacteriol.* 182: 5416–5424.
- Graham A, Mason D, Peck M. 1996. Predictive model of the effect of temperature, pH and sodium chloride on growth from spores of non-proteolytic *Clostridium botulinum*. *Int. J. Food Microbiol.* 31:69–85.
- Grainger DC, Hurd D, Harrison M, Holdstock J, Busby SJW. 2005. Studies of the distribution of *Escherichia coli* cAMP-receptor protein and RNA polymerase along the *E. coli* chromosome. *Proc. Natl. Acad. Sci. U. S. A.* 102:17693–17698.
- Grigorova IL, Phleger NJ, Mutualik VK, Gross CA. 2006. Insights into transcriptional regulation and sigma competition from an equilibrium model of RNA polymerase binding to DNA. *Proc. Natl. Acad. Sci. U. S. A.* 103:5332–5337.
- Grimaud R, et al. 2001. Repair of oxidized proteins. Identification of a new methionine sulfoxide reductase. *J. Biol. Chem.* 276:48915–48920.
- Groisman EA. 1998. The ins and outs of virulence gene expression: Mg²⁺ as a regulatory signal. *Bioessays* 20:96–101.
- Grubbs FE. 1969. Procedures for detecting outlying observations in samples. *Technometrics* 11:1–21.
- Hengge R. 2009. Proteolysis of sigmaS (RpoS) and the general stress response in *Escherichia coli*. *Res. Microbiol.* 160:667–676.
- Hengge-Aronis R. 2002. Recent insights into the general stress response regulatory network in *Escherichia coli*. *J. Mol. Microbiol. Biotechnol.* 4:341–346.
- Hobman JL, Wilkie J, Brown NL. 2005. A design for life: prokaryotic metal-binding MerR family regulators. *Biomaterials* 18:429–436.
- Hoiseth SK, Stocker BAD. 1981. Aromatic-dependent *Salmonella typhimurium* are non-virulent and effective as live vaccines. *Nature* 291: 238–239.
- Holland IB, Jones HE, Campbell AK, Jacq A. 1999. An assessment of the role of intracellular free Ca²⁺ in *E. coli*. *Biochimie* 81:901–907.
- Hornbaek T, Jakobsen M, Dynesen J, Nielsen AK. 2004. Global transcription profiles and intracellular pH regulation measured in *Bacillus licheniformis* upon external pH upshifts. *Arch. Microbiol.* 182:467–474.
- Ibanez-Ruiz M, Robbe-Saule V, Hermant D, Labrude S, Norel F. 2000. Identification of RpoS (σ S)-regulated genes in *Salmonella enterica* serovar Typhimurium. *J. Bacteriol.* 182:5749–5756.
- Ishihama A. 2000. Functional modulation of *Escherichia coli* RNA polymerase. *Annu. Rev. Microbiol.* 54:499–518.

51. Iuchi S, Weiner L. 1996. Cellular and molecular physiology of *Escherichia coli* in the adaptation to aerobic environments. *J. Biochem.* 120: 1055–1063.
52. Iwig JS, Leitch S, Herbst RW, Maroney MJ, Chivers PT. 2008. Ni(II) and Co(II) sensing by *Escherichia coli* RcnR. *J. Am. Chem. Soc.* 130: 7592–7606.
53. Iwig JS, Rowe JL, Chivers PT. 2006. Nickel homeostasis in *Escherichia coli*—the rcnR-rcnA efflux pathway and its linkage to NikR function. *Mol. Microbiol.* 62:252–262.
54. Johnson DC, Dean DR, Smith AD, Johnson MK. 2005. Structure, function, and formation of biological iron-sulfur clusters. *Annu. Rev. Biochem.* 74:247–281.
55. Kanehisa M, Goto S, Kawashima S, Okuno Y, Hattori M. 2004. The KEGG resource for deciphering the genome. *Nucleic Acids Res.* 32: D277–D280.
56. Karavolos M, et al. 2008. Adrenaline modulates the global transcriptional profile of *Salmonella* revealing a role in the antimicrobial peptide and oxidative stress resistance responses. *BMC Genomics* 9:458.
57. Keane OM, Dorman CJ. 2003. The *gyr* genes of *Salmonella enterica* serovar Typhimurium are repressed by the factor for inversion stimulation, Fis. *Mol. Genet. Genomics* 270:56–65.
58. Keseler IM, et al. 2005. EcoCyc: a comprehensive database resource for *Escherichia coli*. *Nucleic Acids Res.* 33:D334–D337.
59. Kisker C, Schindelin H, Rees DC. 1997. Molybdenum-cofactor-containing enzymes: structure and mechanism. *Annu. Rev. Biochem.* 66:233–267.
60. Kjeldgaard NO, Maaloe O, Schaechter M. 1958. The transition between different physiological states during balanced growth of *Salmonella typhimurium*. *J. Gen. Microbiol.* 19:607–616.
61. Klauk E, Typas A, Hengge R. 2007. The sigmaS subunit of RNA polymerase as a signal integrator and network master regulator in the general stress response in *Escherichia coli*. *Sci. Prog.* 90:103–127.
62. Klumpp S, Hwa T. 2008. Growth-rate-dependent partitioning of RNA polymerases in bacteria. *Proc. Natl. Acad. Sci. U. S. A.* 105:20245–20250.
63. Kotlarz D, Garreau H, Buc H. 1975. Regulation of the amount and of the activity of phosphofructokinases and pyruvate kinases in *Escherichia coli*. *Biochim. Biophys. Acta* 381:257–268.
64. Langridge GC, et al. 2009. Simultaneous assay of every *Salmonella* Typhi gene using one million transposon mutants. *Genome Res.* 19: 2308–2316.
65. Le Marc Y, et al. 2008. Modelling the growth of *Clostridium perfringens* during the cooling of bulk meat. *Int. J. Food Microbiol.* 128:41–50.
66. Li S, Cronan JJ. 1993. Growth rate regulation of *Escherichia coli* acetyl coenzyme A carboxylase, which catalyzes the first committed step of lipid biosynthesis. *J. Bacteriol.* 175:332–340.
67. Liu X, Brutlag DL, Liu JS. 2001. BioProspector: discovering conserved DNA motifs in upstream regulatory regions of co-expressed genes. *Pac. Symp. Biocomput.* 6:127–138.
68. Lucchini S, McDermott P, Thompson A, Hinton J. 2009. The H-NS-like protein StpA represses the RpoS (sigma 38) regulon during exponential growth of *Salmonella* Typhimurium. *Mol. Microbiol.* 74:1169–1186.
69. Lucchini S, et al. 2006. H-NS mediates the silencing of laterally acquired genes in bacteria. *PLoS Pathog.* 2:e81.
70. Madigan MT, Martinko JM, Parker J (ed). 2000. Brock biology of microorganisms, p 135–162. Prentice-Hall, Upper Saddle River, NJ.
71. Martin DS. 1932. The oxygen consumption of *Escherichia coli*. *J. Gen. Physiol.* 15:691–708.
72. McHugh JP, et al. 2003. Global iron-dependent gene regulation in *Escherichia coli*—a new mechanism for iron homeostasis. *J. Biol. Chem.* 278:29478–29486.
73. Mellefont LA, Ross T. 2003. The effect of abrupt shifts in temperature on the lag phase duration of *Escherichia coli* and *Klebsiella oxytoca*. *Int. J. Food Microbiol.* 83:295–305.
74. Monod J. 1949. The growth of bacterial cultures. *Annu. Rev. Microbiol.* 3:371–394.
75. Müller M. 1895. Ueber den Einfluss von Fieber temperaturen auf die Wachstums geschwindigkeit und die Virulenz des Typhus Bacillus. *Z. Hyg. Infektionskr.* 20:245.
76. Mulrooney S, Hausinger R. 2003. Nickel uptake and utilization by microorganisms. *FEMS Microbiol. Rev.* 27:239–261.
77. Naseem R, Holland IB, Jacq A, Wann KT, Campbell AK. 2008. pH and monovalent cations regulate cytosolic free Ca^{2+} in *E. coli*. *Biochim. Biophys. Acta* 1778:1415–1422.
78. Navarro Llorens J, Tormo A, Martínez-García E. 2010. Stationary phase in gram-negative bacteria. *FEMS Microbiol. Rev.* 34:476–495.
79. Nilsson L, Vanet A, Vijgenboom E, Bosch L. 1990. The role of FIS in trans activation of stable RNA operons of *Escherichia coli*. *EMBO J.* 9:727–734.
80. Ninnemann O, Koch C, Kahmann R. 1992. The *E. coli* Fis promoter is subject to stringent control and autoregulation. *EMBO J.* 11:1075–1083.
81. Nyström T. 2003. The free-radical hypothesis of aging goes prokaryotic. *Cell. Mol. Life Sci.* 60:1333–1341.
82. Nyström T. 2007. A bacterial kind of aging. *PLoS Genet.* 3:e224.
83. Ono S, et al. 2005. H-NS is a part of a thermally controlled mechanism for bacterial gene regulation. *Biochem. J.* 391:203–213.
84. Osuna R, Lienau D, Hughes KT, Johnson RC. 1995. Sequence, regulation, and functions of Fis in *Salmonella typhimurium*. *J. Bacteriol.* 177: 2021–2032.
85. Outten CE, O'Halloran TV. 2001. Femtomolar sensitivity of metallo-regulatory proteins controlling zinc homeostasis. *Science* 292: 2488–2492.
86. Penfold WJAS. 1914. On the nature of bacterial lag. *J. Hyg. (Lond.)* 14:215–241.
87. Pin C, et al. 2009. Network analysis of the transcriptional pattern of young and old cells of *Escherichia coli* during lag phase. *BMC Syst. Biol.* 3:108.
88. Ponce E, Flores N, Martinez A, Valle F, Bolívar F. 1995. Cloning of the two pyruvate kinase isoenzyme structural genes from *Escherichia coli*: the relative roles of these enzymes in pyruvate biosynthesis. *J. Bacteriol.* 177: 5719–5722.
89. Potrykus K, Cashel M. 2008. (p)ppGpp: still magical? *Annu. Rev. Microbiol.* 62:35–51.
90. Prinz WA, Aslund F, Holmgren A, Beckwith J. 1997. The role of the thioredoxin and glutaredoxin pathways in reducing protein disulfide bonds in the *Escherichia coli* cytoplasm. *J. Biol. Chem.* 272:15661–15667.
91. Proshkin S, Rahmouni A, Mironov A, Nudler E. 2010. Cooperation between translating ribosomes and RNA polymerase in transcription elongation. *Science* 328:504–508.
92. Py B, Moreau PL, Barras F. 2011. Fe-S clusters, fragile sentinels of the cell. *Curr. Opin. Microbiol.* 14:218–223.
93. Radonjic M, et al. 2005. Genome-wide analyses reveal RNA polymerase II located upstream of genes poised for rapid response upon *S. cerevisiae* stationary phase exit. *Mol. Cell* 18:171–183.
94. Ramseier TM, Saier MH, Jr. 1995. cAMP-cAMP receptor protein complex: five binding sites in the control region of the *Escherichia coli* mannitol operon. *Microbiology* 141:1901–1907.
95. Rodionov DA, Hebbeln P, Gelfand MS, Eitinger T. 2006. Comparative and functional genomic analysis of prokaryotic nickel and cobalt uptake transporters: evidence for a novel group of ATP-binding cassette transporters. *J. Bacteriol.* 188:317–327.
96. Rodrigue A, Boxer DH, Mandrand-Berthelot MA, Wu LF. 1996. Requirement for nickel of the transmembrane translocation of NiFe-hydrogenase 2 in *Escherichia coli*. *FEBS Lett.* 392:81–86.
97. Ross W, Thompson JF, Newlands JT, Gourse RL. 1990. *Escherichia coli* Fis protein activates ribosomal-RNA transcription *in vitro* and *in vivo*. *EMBO J.* 9:3733–3742.
98. Saint-Ruf C, Pesut J, Sopta M, Matic I. 2007. Causes and consequences of DNA repair activity modulation during stationary phase in *Escherichia coli*. *Crit. Rev. Biochem. Mol. Biol.* 42:259–270.
99. Sambrook J, Russell D. 2000. Molecular cloning. Cold Spring Harbor Laboratory Press, Cold Spring Harbor, NY.
100. Scamuffa MD, Caprioli RM. 1980. Comparison of the mechanisms of two distinct aldolases from *Escherichia coli* grown on gluconeogenic substrates. *Biochim. Biophys. Acta* 614:583–590.
101. Schaechter M, Maaloe O, Kjeldgaard NO. 1958. Dependency on medium and temperature of cell size and chemical composition during balanced growth of *Salmonella typhimurium*. *J. Gen. Microbiol.* 19: 592–606.
102. Sezonov G, Joseleau-Petit D, D'Ari R. 2007. *Escherichia coli* physiology in Luria-Bertani broth. *J. Bacteriol.* 189:8746–8749.
103. Shultzaberger RK, Chen Z, Lewis KA, Schneider TD. 2007. Anatomy of *Escherichia coli* sigma70 promoters. *Nucleic Acids Res.* 35:771–788.
104. Swinnen IAM, Bernaerts K, Dens EJJ, Geeraerd AH, Van Impe JF. 2004. Predictive modelling of the microbial lag phase: a review. *Int. J. Food Microbiol.* 94:137–159.
105. Thompson A, et al. 2006. The bacterial signal molecule, ppGpp, medi-

- ates the environmental regulation of both the invasion and intracellular virulence gene programs of *Salmonella*. *J. Biol. Chem.* 281:30112–30121.
106. Thompson A, Rowley G, Alston M, Danino V, Hinton JC. 2006. *Salmonella* transcriptomics: relating regulons, stimulons and regulatory networks to the process of infection. *Curr. Opin. Microbiol.* 9:109–116.
 107. Touati D. 2000. Iron and oxidative stress in bacteria. *Arch. Biochem. Biophys.* 373:1–6.
 108. Tree JJ, Kidd SP, Jennings MP, McEwan AG. 2005. Copper sensitivity of *cueO* mutants of *Escherichia coli* K-12 and the biochemical suppression of this phenotype. *Biochem. Biophys. Res. Commun.* 328:1205–1210.
 109. Tsolis RM, Baumler AJ, Stojiljkovic I, Heffron F. 1995. Fur regulon of *Salmonella typhimurium*: identification of new iron-regulated genes. *J. Bacteriol.* 177:4628–4637.
 110. Vacic V, Iakoucheva LM, Radivojac P. 2006. Two Sample Logo: a graphical representation of the differences between two sets of sequence alignments. *Bioinformatics* 22:1536–1537.
 111. Veit A, Polen T, Wendisch VF. 2007. Global gene expression analysis of glucose overflow metabolism in *Escherichia coli* and reduction of aerobic acetate formation. *Appl. Microbiol. Biotechnol.* 74:406–421.
 112. Velayudhan J, Castor M, Richardson A, Main-Hester KL, Fang FC. 2007. The role of ferritins in the physiology of *Salmonella enterica* sv. Typhimurium: a unique role for ferritin B in iron-sulfur cluster repair and virulence. *Mol. Microbiol.* 63:1495–1507.
 113. Vemuri G, Altman E, Sangurdekar D, Khodursky A, Eiteman M. 2006. Overflow metabolism in *Escherichia coli* during steady-state growth: transcriptional regulation and effect of the redox ratio. *Appl. Environ. Microbiol.* 72:3653–3661.
 114. Visick JE, Cai H, Clarke S. 1998. The L-isoaspartyl protein repair methyltransferase enhances survival of aging *Escherichia coli* subjected to secondary environmental stresses. *J. Bacteriol.* 180:2623–2629.
 115. Wagner R. 1994. The regulation of ribosomal-RNA synthesis and bacterial-cell growth. *Arch. Microbiol.* 161:100–109.
 116. Wang S, Wu Y, Outten FW. 2011. Fur and the novel regulator YqjI control transcription of the ferric reductase gene *yqjH* in *Escherichia coli*. *J. Bacteriol.* 193:563–574.
 117. Wanner BL. 1996. Phosphorus assimilation and control of the phosphate regulon, p 1357–1381. In Neidhardt FC, et al (ed), *Escherichia coli and Salmonella: cellular and molecular biology*, 2nd ed, vol 1. ASM Press, Washington, DC.
 118. Wassarman KM, Saecker RM. 2006. Synthesis-mediated release of a small RNA inhibitor of RNA polymerase. *Science* 314:1601–1603.
 119. Wilson PDG, et al. 2003. Batch growth of *Salmonella typhimurium* LT2: stoichiometry and factors leading to cessation of growth. *Int. J. Food Microbiol.* 89:195–203.
 120. Wright J, et al. 2009. Multiple redundant stress resistance mechanisms are induced in *Salmonella enterica* serovar Typhimurium in response to alteration of the intracellular environment via TLR4 signalling. *Microbiology* 155:2919–2929.
 121. Zbell A, Benoit S, Maier R. 2007. Differential expression of NiFe uptake-type hydrogenase genes in *Salmonella enterica* serovar Typhimurium. *Microbiology* 153:3508–3516.